Continental Shelf Research 68 (2013) 51–66

Contents lists available at ScienceDirect

Continental Shelf Research

journal homepage: www.elsevier.com/locate/csr

Research papers

Suspended matter mean distribution and seasonal cycle in the Río de La Plata estuary and the adjacent shelf from ocean color satellite (MODIS) and *in-situ* observations

Diego Moreira [a,*], Claudia G. Simionato [a], Francis Gohin [b], Florence Cayocca [b], Moira Luz Clara Tejedor [a]

[a] Centro de Investigaciones del Mar y la Atmósfera (CIMA/CONICET-UBA), Instituto Franco-Argentino para el Estudio del Clima y sus Impactos (UMI IFAECI/CNRS-CONICET-UBA), Departamento de Ciencias de la Atmósfera y los Océanos, FCEN, Universidad de Buenos Aires, Argentina
[b] Institut Français de Recherche pour l'Exploitation de la Mer (IFREMER), France

ARTICLE INFO

Article history:
Received 12 November 2012
Received in revised form
6 August 2013
Accepted 26 August 2013
Available online 2 September 2013

Keywords:
In-situ observations
Turbidity
Seasonal variability
Sedimentological processes
MODIS
OC5 Algorithm

ABSTRACT

The Río de la Plata is one of the largest and most turbid estuaries of the world, carrying a total of 160 million tons y^{-1} of suspended sediments. The knowledge of their spatial distribution and their scales of variability is fundamental for management and scientific reasons, but has been limited by the scarcity of observations. During 2009 and 2010, *in-situ* data (CTD and turbidity profiles, and water and bottom sediment samples) were collected at 26 sites during six repeated cruises and from three fixed instruments deployed in the frame of the FREPLATA/FFEM experiment. In this paper we complement the analysis of this *in-situ* data base with 10 years of daily intermediate resolution (1 km) MODIS-Aqua observations processed for surface suspended matter using the IFREMER algorithm for coastal turbid waters. The aim of this work is to provide a comprehensive characterization of the annual mean suspended matter concentration distribution, to study its variability on seasonal time scale and to identify the involved physical mechanisms. The comparison between the statistics of the direct and remote sensed data is satisfactory, showing a good agreement in the magnitude and spatial distribution of the mean suspended sediments concentration, its standard deviation, so as the seasonal variability. Our data show that all along the year the concentration of surface suspended matter maximizes along the southern coast of the upper and intermediate estuary and at the tips of Samborombón Bay. This fact is linked in part with the higher solid discharge of the Paraná River – flowing along the southern coast – compared to the Uruguay River which flows following the northern coast. The former receives most of the sediments load to the Río de la Plata from the Bermejo River. The observed mean pattern is also related to the stronger tidal currents along the southern coast of the estuary and at the tips of Samborombón Bay, which act re-suspending sediments near the bottom. Then, wind waves during storms enhance vertical mixing, increasing the surface concentration. The concentration of suspended sediments rapidly falls seawards the Barra del Indio shoal, in the area of the salt wedge. In the outer estuary, suspended matter concentration is also strongly associated to the wind-forced motion of the freshwater plume. Suspended matter concentration exhibits a maximum in winter and a minimum in summer, that cannot be fully explained in terms of the seasonal cycle of the solid discharge of the tributaries, but seems to be related to a raise in the frequency of the storms in winter, increasing the frequency of strong winds and higher wind waves, and the associated re-suspension and mixing.

1. Introduction

With a length of 320 km and a width more than 200 km at its mouth, the Río de la Plata (RDP, Fig. 1) is an extensive and shallow (<20 m) estuary, located in the eastern coast of South America at approximately 35°S. It drains the second largest basin of South America, formed by the Paraná and the Uruguay rivers. They contribute to a joint mean runoff of 22,000 $m^3 s^{-1}$, even though peaks as highs as 80,000 $m^3 s^{-1}$ and as low as 8000 $m^3 s^{-1}$ have been observed in association with the El Niño – Southern Oscillation cycles (Robertson and Mechoso, 1998; Jaime and Menéndez, 2002). Besides its geographical extension, the estuary is of large social, ecological and economical importance for the countries on its shores (Argentina and Uruguay). The capital cities of both countries (Buenos Aires and Montevideo) and a number of harbors, resorts and

* Correspondence to: Intendente Güiraldes 2160 – Ciudad Universitaria, Pabellón II – 2do. Piso, (C1428EGA) Ciudad Autónoma de Buenos Aires, Argentina. Tel.: +54 11 4787 2693, +54 11 4576 3300/09x388; fax: +54 11 4788 3572.
E-mail address: moreira@cima.fcen.uba.ar (D. Moreira).

0278-4343/$ - see front matter © 2013 Elsevier Ltd. All rights reserved.
http://dx.doi.org/10.1016/j.csr.2013.08.015

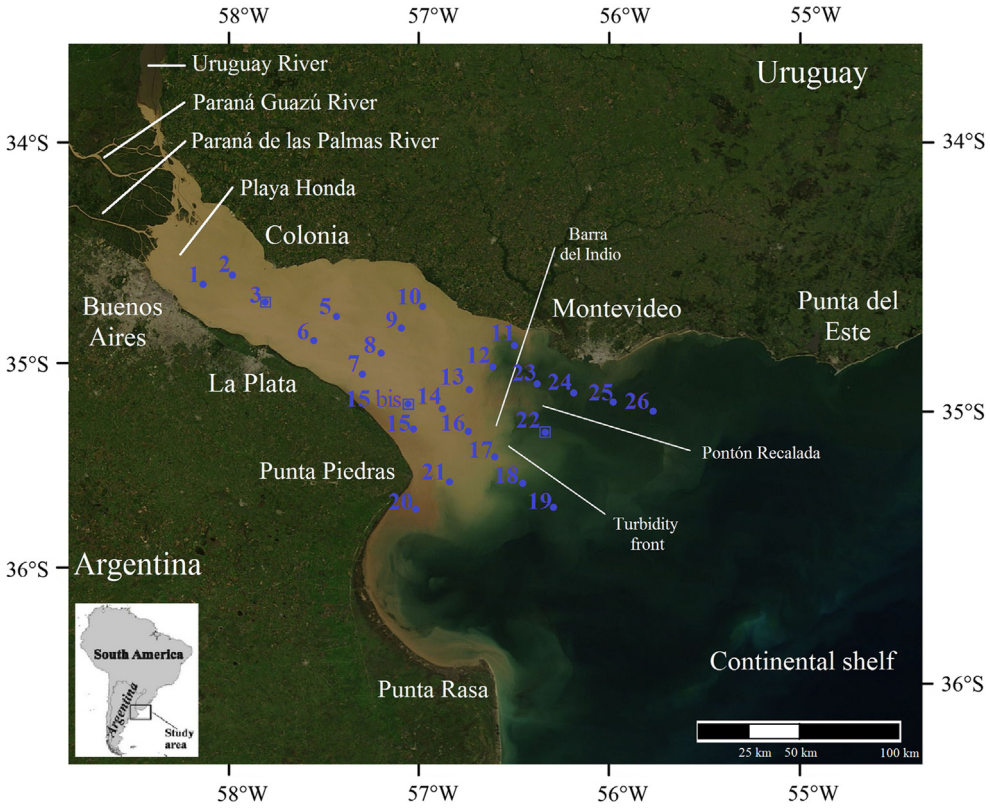

Fig. 1. Study area and geographical references superimposed over a true color MODIS image from Visible Earth (http://visibleearth.nasa.gov). Blue dots indicate the 26 sampling sites during the oceanographic cruises, whereas blue squares show the location of the fixed instruments. (For interpretation of the references to color in this figure legend, the reader is referred to the web version of this article.)

industrial centers are located on its margins and influence zone. The estuary constitutes the main source of drinking water for the millions of inhabitants in the region, for whom it is also an important recreational area. The RDP is rich in nutrients and, therefore, has an abundant and diverse fauna. It has important fisheries and has the unusual feature of being a spawning and nursery area for several coastal species (Cousseau, 1985; Boschi, 1988; Macchi et al., 1996; Acha et al., 1999; Acha and Macchi, 2000; Berasategui et al., 2004, 2006; Rodrigues, 2005). The life cycles of these fishes seem to be strongly linked with turbidity (Jaureguizar et al., 2003a, 2003b, Dogliotti et al., 2011). This association is not completely understood yet, but it could be connected to feeding benefits due to an increase of prey abundance due in part to the retentive properties of the system (Simionato et al., 2008, Acha et al., 2012), or to protection from avian predation (Jaureguizar et al., 2003a, 2003b). Samborombón Bay is one of the most important wetlands of Argentina and is home to a number of species of fishes, turtles, crabs and migratory birds (Lasta, 1995; Canevari et al., 1998). The fresh water plume of the RDP impacts the shelf in a distance of more than 500 km (Campos et al., 1999).

The sedimentological features of the RDP have been described by Ottmann and Urien (1966), Urien (1972), Ayup (1986, 1987), Parker et al. (1986a, 1986b, 1987), Cavallotto (1987), López Laborde (1987, 1997), Parker and López Laborde (1988, 1989), López Laborde and Nagy (1999), Guarga et al. (1991) and Cavallotto and Violante (2008). The sediments that reach the estuary come mainly from the Paraná River and from the drainage of a number of small tributaries along the Argentinean coast. These rivers, carry high amounts of nutrients, suspended particulate and dissolved organic matter to the estuary and, therefore, to the adjacent shelf waters. The amount of sediments transported by the RDP has been estimated in more than 160 million tons y^{-1} (Simionato et al., 2011b). As a consequence, it is one of the most turbid estuaries in the world, with extreme concentrations more than 400 g m^{-3} (Framiñan and Brown, 1996).

The issue is important because many environmental questions in the RDP and the adjacent shelf are linked to the high sediments load of this estuary. The most significant topics include optimization of dredging operations (Cardini et al., 2002), understanding geomorphological change (Codignotto et al., 2012; Dragani et al., 2012), contamination (Colombo et al., 2005, 2007), bentonic ecology (Gomez-Erache et al., 1999), primary productivity (Gómez-Erache et al., 2004; Huret et al., 2005), fisheries (Jaureguizar et al., 2003a, 2003b, 2008), evaluating fluxes of particulate organic carbon to the sea and biogeochemical modeling (Huret et al., 2005). Nevertheless, the problem of the suspended sediments in estuaries and coastal seas is intrinsically difficult, because sedimentological processes are not only numerous and complex but also highly site dependent and variable over a broad spectrum of time and space scales. This variability renders the most traditional field sampling methods as inadequate in studies to resolve sediment dynamics in complex coastal waters (Miller and McKee, 2004).

In the particular case of the RDP, the lack of observations has been historically the main limitation to the knowledge of the sedimentological processes. The previous works which dealt with the suspended matter (SM) distribution and the involved physical processes in the estuary have been summarized by López Laborde and Nagy (1999). Most of what is known is based on the work by Ottmann and Urien (1966), who analyzed data collected along three legs across the very upper estuary, one leg along the navigation channel from Buenos Aires to Pontón Recalada and three legs at the exterior estuary, from Punta Rasa to Punta del Este. Based on those observations the authors classified the RDP into three geographical zones, which they postulated corresponded to three different sedimentological regimes: (i) an upper zone, upstream

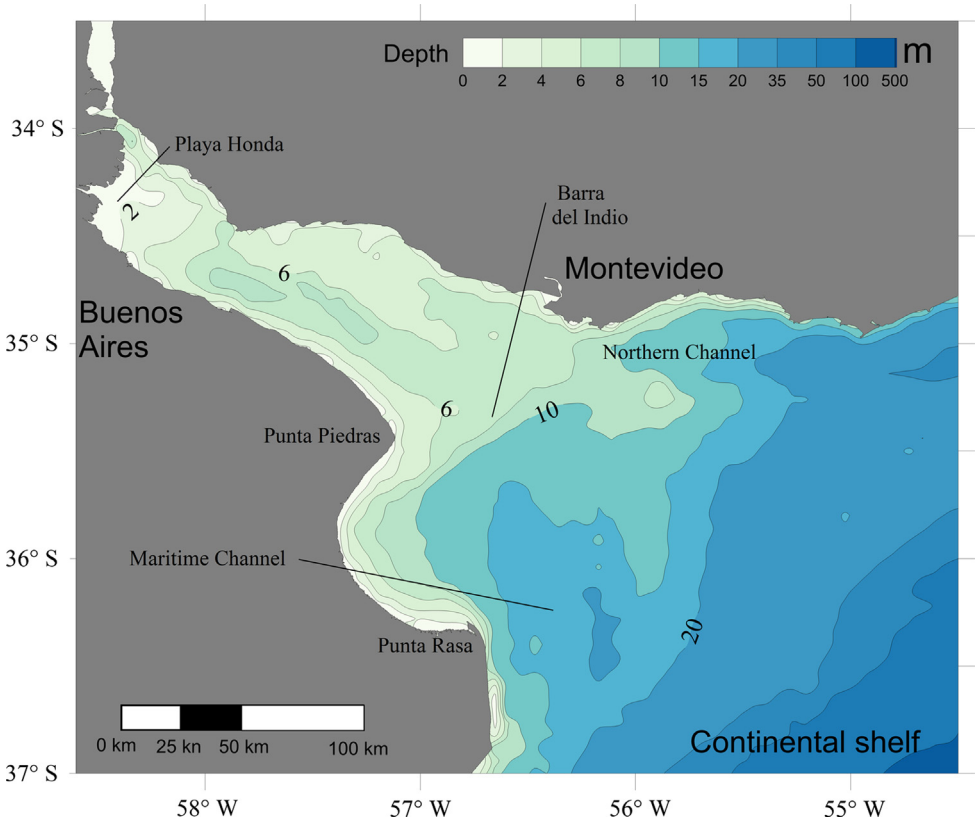

Fig. 2. Bathymetry of the Río de la Plata estuary (m). From the FREPLATA Project collected by digitalization of the nautical charts (H1, H117 and H118).

the line Buenos Aires-Colonia, comprising the Paraná River Delta front and its sub-aqueous extension (Playa Honda), which they defined as a typical sedimentation area of a fluvial delta; (ii) an intermediate zone, comprising the area between the line Buenos Aires-Colonia to almost Punta Piedras-Montevideo, which they defined as a fluvial zone where the transport of suspended sediments "predominates"; (iii) an outer zone, up to the line Punta del Este-Punta Rasa, which is the area of greater salinity variation and where sedimentation processes would "actually take place". The authors pointed out an increasing SM concentration to the southeast and an asymmetrical distribution along the Uruguayan and Argentinean coasts of the RDP, showing greater values over the southern than over the northern region. They mention a number of processes which might be responsible for the observed features: flocculation, river discharge and wave and tidal current resuspension. They deduced that a maximum turbidity zone should occur in the exterior estuary; it was confirmed by later studies (Framiñan and Brown, 1996; Framiñan et al., 1999). Urien (1972) affirmed that the sedimentological pattern in the RDP would be primary controlled by the estuarine environment. In the upper and intermediate estuary, fluvial fresh water conditions would exist. There, "tides and waves from the East" would "control the sediment dispersion". In the exterior estuary the bulk of fluvial discharge would "flow mainly through the northern channel", whereas the shallowness of Bahía de Samborombón would "protect it from wave and current action" and would favor the deposition of fine sediments. Ayup (1986, 1987) stated that in the exterior estuary the sedimentological processes would be strongly associated with the stratification; the occurrence of a halocline would favor flocculation and aggregation. This way, even though a basic knowledge of the spatial SM distribution and its potential forcings exists, many aspects are still unclear. Actually, the scarcity of observations did not even permit the determination of representative annual mean values. Moreover, almost nothing is known about the temporal scales of variability.

In this sense, between November 2009 and December 2010, the FREPLATA/FFEM (Environmental Protection of the Río de la Plata and its Maritime Front / French Fund for the Global Environment) Experiment was performed with the aim of gathering a new and rich *in-situ* data base of hydro-sedimentological variables to aid in the understanding and numerical modeling of the underlying processes (Simionato et al., 2011a; Simionato et al., 2011b). The experiment included six cruises with 26 oceanographic stations each, where temperature, conductivity and turbidity profiles were measured and surface and bottom water samples were collected. Simultaneously, fixed instruments measuring waves, temperature, conductivity and turbidity were deployed at three sites of the estuary. One of these instruments also recorded meteorological variables.

Even though the efforts made during the FREPLATA/FFEM experiment represent a large improvement to the previous scarcity of data in the RDP, many more observations are necessary to study the high SM concentration variability observed in this system. In this sense, even though ocean color satellite observations are highly contaminated by the presence of clouds, they supply data with high temporal and spatial resolution, which can provide a synoptic view of the variables and which permit the analysis of their spatio-temporal variability (Miller and McKee, 2004). The attractiveness of remote sensing as an information source has increased greatly over the last ten years as the new generation of satellite sensors has become available. In particular, more than 10 years of continuous observations at medium resolution (1 km) are available from the MODIS-Aqua (Moderate Resolution Imaging Spectroradiometer on board of the Aqua satellite) mission, becoming a unique source of data over a considerable large period of time. Total SM data for the RDP and the adjacent ocean have been derived by the French Research

Institute for the Exploitation of the Sea (IFREMER) from the MODIS-Aqua observations, using algorithms and methods established for the Bay of Biscay and the English Channel (Gohin et al., 2005, Gohin, 2011) and used after validation on the European North-West shelf, including the turbid coastal waters of the United-Kingdom (Sykes and Barciela, 2012).

The aim of this paper is to analyze the above described complementary sets of *in-situ* and remote data, to provide a comprehensive characterization of the annual mean SM concentration distribution in the RDP and the adjacent shelf, to study its variability on seasonal time scale and to identify the involved physical mechanisms. This knowledge is indispensable as a first step in the construction and validation of numerical models, which are needed for management and scientific purposes in this socially, economically and ecologically important region.

2. Study area

The RDP (Fig. 1) has a northwest to southeast oriented funnel shape approximately 300 km long that narrows from 220 km at its mouth to 40 km at its upper end (Balay, 1961). The estuarine area is 35,000 km^2 and the fluvial drainage area is 3.1×10^6 km^2 (Depetris and Griffin, 1968).

This estuary has a complex geometry and bathymetry (Fig. 2). A complete description of its morphology can be found in Ottman and Urien (1965, 1966), Urien (1966, 1967, 1972), Depetris and Griffin (1968), Parker et al. (1986a, 1986b) and López Laborde (1987). The estuary is divided into two regions by the Barra del Indio shoal, a shallow area (7–10 m) that crosses the estuary following a line between Punta Piedras and Montevideo (Fig. 2). The upper region is mainly occupied by fresh water; except for a few coastal channels, depths in this area are less than 7 m. Seawards the shoal is the Maritime Channel, a wide depression with depth between 12 and 20 m. Samborombón Bay is a very shallow and extensive area with depths ranging from 2 to 10 m extending south of Punta Piedras.

The estuary is a micro-tidal system. Tidal waves associated with the South Atlantic amphidromes reach the Continental Shelf while propagating northward (O'Connor, 1991; Glorioso and Flather, 1995, 1997; Simionato et al., 2004a). As they propagate over the shelf, geographic setting modifies their propagation so that they enter the estuary mainly from the southeast (Simionato et al., 2004a). The shallow water shortens the wavelength after they enter the estuary; owing to this effect and the considerable length of the estuary, semidiurnal constituents have the unusual feature of nearly complete a wavelength within the estuary at all times (CARP, 1989). Tidal amplitudes are generally not amplified toward the upper part. The estuary is long and converges only at its innermost part, where it is extremely shallow and bottom friction plays a fundamental role in controlling the wave amplitude (Simionato et al., 2004a). The tidal regime in the estuary is mixed, dominantly semidiurnal, with M_2 being the most significant constituent (M_2 has an amplitude of 0.27 m at Buenos Aires); however, there are significant diurnal inequalities, mostly caused by O_1, with an amplitude of 0.15 m at Buenos Aires (D'Onofrio et al., 1999).

Given that water level is easier to measure than tidal currents, observations of this last variable are scarcer, and much of what is known about its behavior was inferred from numerical simulations. Maximum speeds occur at the northernmost and southernmost limits of Samborombón Bay whereas in its interior they are weaker. This last region displays a rotational feature, but at the upper and central estuary tidal currents tend to be more unidirectional; this last is also the case along the Uruguayan coast (Simionato et al., 2004a).

The liquid discharge to the RDP is determined by the Paraná and Uruguay rivers in more than 97% (Bombardelli et al., 1995; Framiñan et al., 1999) and displays a weak seasonal cycle with a maximum in winter of around 30,000 $m^3 s^{-1}$ and a minimum in summer of approximately 20,000 $m^3 s^{-1}$ (Nagy et al., 1997; Simionato et al., 2001). Nevertheless, the solid load to the estuary mostly depends upon the input of one of the tributaries to the Paraná River, called Bermejo River (INA, 2010), which in fact gets its name ('Bermejo' means 'Red' in Castilian) from the color of the sediments that it transports. This river's contribution is about 75% of the solid load of the Paraná River, and is composed in a 75% of fine sediments – clays and especially silts – and 25% of sand (Simionato et al., 2011b). Because of this reason, the seasonal cycle of the solid discharge to the RDP depends upon the cycles of the Bermejo River and is not only connected to the liquid discharge of the main tributaries. Even though there are not continuous measurements of the solid runoff to the RDP, the discharge of the Bermejo River before it reaches the Paraná River has been measured at El Colorado station, located at 26° 20′ 03.40″ S and 59° 21′ 44.70′ W during many years (http://www.hidricosargentina.gov.ar/acceso_bd.php).

The atmospheric general circulation in the RDP region is controlled by the influence of the quasi-permanent South Atlantic high-pressure system. Southwestward circulation, associated with this high, advects warm and moist air from subtropical regions over the estuary (Minetti and Vargas, 1990). On the other hand, cold systems coming from the south drive cold and dry air masses over the area with a dominant periodicity of around 4 days (Vera et al., 2002). As a result, an alternation of winds from the northeast to the southwest in a scale of a few days is the dominant feature of wind variability in the area. Due to the highest frequency of storms in the cold season, northeasterlies are dominant in spring-summer, whereas southwesterlies are more frequent in fall-winter (Simionato et al., 2005a). This wind variability strongly influences currents and stratification in the estuary (Simionato et al., 2004b, 2005b, 2006, 2007, 2010; Meccia et al., 2009, 2013).

Density in the RDP is controlled by salinity, whereas changes in temperature, even important from one season to another, only display small horizontal gradients (Guerrero et al., 1997). Water stratification is controlled by the confluence of highly buoyant continental discharge advecting offshore, lying on denser shelf waters that intrude into the estuary as a topographically controlled (by the Barra del Indio shoal) salt wedge. This salt wedge is typically between 100 and 250 km long (Guerrero et al., 1997) and defines a bottom salinity front, over the Barra del Indio shoal following approximately the 10 m isobath (Guerrero et al., 1997). Forced by the prevailing winds (Simionato et al., 2001) both surface and bottom salinity fronts show a seasonal cycle that largely modifies the salt wedge structure from spring-summer to fall-winter (Guerrero et al., 1997). Over long-term time scales, a spatial overlap has been observed between this bottom salinity front and the maximum turbidity zone (Framiñan and Brown, 1996).

The estuary has been historically divided in three regions. The upper estuary, close to the mouth of the main tributaries, has a mostly fluvial regime. The intermediate estuary is the zone upstream the Barra del Indio shoal, where water is most of the time fresh, but is intruded by ocean salty water. The lower estuary, seawards the Barra del Indio, has a dominant oceanic regime, but is influenced by the buoyant fresh plume of the estuary (see Framiñan et al., 1999 and references therein).

3. Data and methods

3.1. In-situ observations from the FREPLATA/FFEM experiment

In the frame of the FREPLATA Project, and funded by the French Fund for the Global Environment (FFEM), a data acquisition campaign was performed in the RDP (FREPLATA/FFEM Experiment,

Simionato et al., 2011a; 2011b) as a cooperation among several Argentinean, Uruguayan and French institutions. During 2009 and 2010, six oceanographic synoptic cruises were done every approximately 2 months: in November 2009 and March, June, August, October and December 2010. During each cruise CTD (conductivity–temperature–depth) and turbidity profiles and water and bottom sediment samples were gathered during a period of 2–3 days at the 26 sites shown as dots in Fig. 1. Complete information about the data and the procedures applied to the samples can be found in Simionato et al. (2011a, 2011b), but the most important aspects will be summarized in what follows.

The CTD was a "Seabird", model SBE-19; a "Campbell Scientific" OBS3+ turbidimeter (NS 8226) was attached to it. The sampling frequency was 2 Hz what, at a downcast speed of 0.3–0.5 m s^{-1} resulted on a vertical resolution of 4–7 data per meter. The CTD was operated in real time using an interface SBE NS 0128. The heart of the OBS3+ sensor is a near infrared laser and photodiode for detecting the intensity of light scattered from suspended particles in water. The sensor was calibrated by the manufacturer.

At every oceanographic station, water samples were collected with a pump with the aim of calibrating the conductivity (with an Autosal Guidline at the laboratory) and turbidity sensors. The samples' turbidity was measured *in-situ* using a "HACH" 2100 P ISO portable turbidimeter with a range of 0–1000 NTU. Additionally, one liter samples of near surface water were gathered for the determination of the SM concentration at every station. These samples were analyzed by the Hydrographic Service of the Navy of Argentina. Once at the laboratory, the samples were filtered (diameter: 47 mm; pore: 0.45 μm), dried at 40 °C for 12 h, kept in a drying cabinet until they cooled, and then weighed for the determination of the SM concentration. Several replicates at random of the samples were done for every cruise. The difference between replicates (accuracy) resulted less than 5%.

This way, after samples' laboratory analysis and data processing, six temperature, salinity and turbidity profiles, so as surface SM and turbidity observations from the water samples were available at each of the 26 sites. These data provide a synoptic view of the mentioned fields so as information about the seasonal variability.

Simultaneously, fixed instruments measured high temporal resolution time series of diverse variables in three sites; two of them correspond to the Pilote Norden and Torre Oyarvide towers and the third was close to Pontón Recalada with an oceanographic buoy. The locations of the instruments were indicated as squares in Fig. 1. The instruments fixed to Pilote Norden and Torre Oyarvide recorded pressure (for waves), temperature, conductivity and turbidity every 15 min during approximately 1 and 2 months, respectively. In Pontón Recalada hourly meteorological observations and water temperature, conductivity and turbidity data were gathered during one year.

At all the three stations an "NKE" SMATCH TT multiparameter probe was used; it included a "Seapoint" turbidimeter. These last instruments were calibrated with formazin at the laboratory before every cruise. In Pilote Norden and Torre Oyarvide the probe also included a pressure sensor SP2T30-PR of "NKE" for waves' observation.

3.2. MODIS-aqua suspended matter data

Daily standard remote-sensing reflectances of MODIS-Aqua have been used in this study. The MODIS Level-2 reflectance products have been downloaded in near real time from the OceanColor/GSFC (Goddard Space Flight Centre, http://modis.gsfc.nasa.gov).

The temporal resolution is of one day, the horizontal resolution of 1 km and data collection spans the period August 8th 2002 to August 23th 2012. The normalized remote-sensing reflectances were processed by IFREMER for estimating Chlorophyll-*a* (Chl-*a*) concentration and non-algal suspended matter (SM) using algorithms and methods established for the Bay of Biscay and the English Channel (Gohin et al., 2005, Gohin, 2011) and used after validation on the European North-West shelf, including the turbid coastal waters of the United Kingdom (Sykes and Barciela, 2012).

The non-algal SM is defined as the difference between total suspended matter and phytoplankton biomass, the latter derived from Chl-*a*. The estimation of Chl-*a* is obtained by application of a satellite-specific lookup table to the spectral remote-sensing reflectance or *Rrs* (Gohin et al., 2002). In coastal waters, non-algal SM, absorption by colored dissolved organic matter (CDOM), and errors in the atmospheric correction are the causes of frequent overestimations in the Chl-*a* concentration by the standard procedures. To estimate the chlorophyll concentration, the OC5 algorithm considers four channels ranging from 442 (blue) to 559 (green), like the OC4 NASA (National Aeronautics and Space Administration) algorithm, but also makes use of the reflectance at 412 nm. Chl-*a* concentration is determined from the triplet {*Rrs*(412), *Rrs*(green), maximum band ratio *Rrs*(blue)/*Rrs*(green)}. *Rrs*(412) accounts for the absorption by CDOM and the error in atmospheric correction, particularly significant at this low wavelength, and *Rrs*(green) accounts for the effect of the backscattering by the suspended sediment not related to the phytoplankton (Gohin et al., 2005). Knowing that CDOM can be neglected at wavelength longer than 550 nm, Gohin et al. (2005) proposed a simple equation to express the reflectance from the absorption (a) and backscattering (b_b) coefficients of pure water, phytoplankton (or Chl-*a*) and SM. They defined a linear relationship between a variable linked to the under-water reflectance, $R^*(550)$, and the normalized remote-sensing reflectance *Rrs*:

$$R^*(550) = b_b/(a+b_b) = \alpha + \beta\, Rrs(550)$$

where α and β are constants whose determination is detailed in Gohin et al. (2005). After making some common hypotheses on a linear contribution of SM to absorption and backscattering, the concentration of SM, SM(550), is obtained by inverting $R^*(550)$.

After having observed a significant under-estimation by our initial method based on the green channel alone, at 550 nm, in the most turbid areas of the Bay of Biscay (Petus et al. 2010), the remote-sensing reflectance at 670 nm has been added to the procedure (Gohin, 2011). This limitation of the SM(550) procedure is due to the fact that the remote-sensing reflectance tends to saturate at lower turbidity for smaller wavelengths (Bowers et al., 1998; Nechad et al., 2010).

To cope with the estimation of SM in areas of variable turbidity, SM(550) or SM(670) is chosen depending on the retrieved levels. In practice, if SM(550) and SM(670) are both inferior to 4 g m^{-3}, then SM(550) is conserved; otherwise, SM(670) is chosen. Therefore, SM is obtained from the channel at 550 nm for clear waters and from the channel at 670 nm in turbid waters. A strict flagging is applied to the data through the NASA flags: HITAU (High aerosol optical thickness), ATMWARN (suspect atmospheric correction) and HILT (High Radiance). As the saturation effect can also limit the validity of SM(670) in the highly turbid waters, the values superior to 98 g m^{-3} have been flagged in our procedure. In consequence, for the RDP, the great majority of the SM is calculated from the channel at 670 nm. It must be noted that there is a possible negative bias of our method in the most turbid areas as the highest concentrations of SM tend to be flagged (ATMWARN and HILT flags, retrieved values superior to 98 g m^{-3}, failure in the standard atmospheric correction; Dogliotti et al., 2011). On average, over the area considered, 28% of the days have a valid observation.

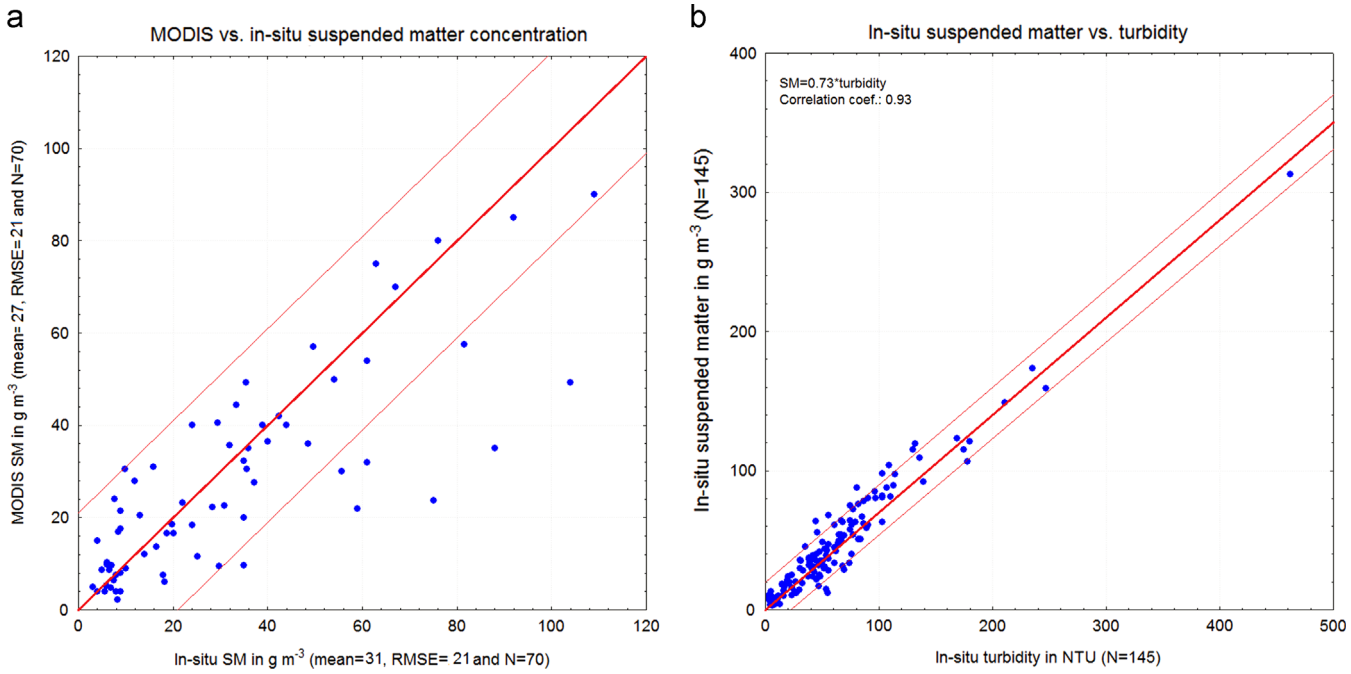

Fig. 3. (a) Scatter plot of remote (MODIS-Aqua, g m^{-3}) *vs. in-situ* SM concentration observations (g m^{-3}); (b) scatter plot of *in-situ* SM concentration (g m^{-3}) *vs. in-situ* turbidity (NTU) from the water samples collected during the six FREPLATA/FFEM experiment cruises.

To analyze the remote data quality, Fig. 3a shows a scatter plot of the remote (MODIS-Aqua) *vs. in-situ* SM observations. This figure was built by assigning to every SM *in-situ* observation derived from the water samples collected during the six FREPLATA/FFEM Experiment quasi-synoptic cruises, an average of the available MODIS-Aqua data from one day before to one day after the period of each cruise. This way the comparison has several limitations that must be taken into account when analyzing the plot. The most important of them is the fact that the MODIS-Aqua mean and the *in-situ* data do not necessarily represent to the same instant; this way, there is a potential effect of tides and winds on *in-situ vs.* remote data dispersion. Also, whereas the remote-sensing method actually sample varying depths, inversely related to the surface turbidity, the *in-situ* samples are taken at fixed depth. Results show that the *in-situ* SM mean was 31 g m^{-3}, whereas the MODIS-Aqua SM mean is somewhat lower, of 27 g m^{-3}, showing a general trend of the satellite observations to underestimate the *in-situ* values. The figure also suggests that the underestimation would be larger for higher SM concentrations, even though it cannot be fully assessed with the number of samples available. Nevertheless, the correlation coefficient resulted of 0.81, what is significant at a 95% level. We conclude that for a better estimation of SM in these areas the channels at longer wavelength (865 nm) should be used.

3.3. Multi-channel singular spectral analysis

In this work we apply multi-channel singular spectral analysis (MSSA) to the observations. Complete descriptions of the statistical method, its application to geophysical signals and the involved theory can be found in Ghil et al. (2002) and Morala et al. (2003), among others. MSSA is an extension of the singular spectral analysis (SSA) to a set of series and can be used to identify and to reconstruct the common underlying oscillatory components of the time series. This methodology combines two useful features: (i) it determines the data set's major directions in phase space – *i.e.*, the directions of dominant variability – with the help of principal component analysis; and (ii) it extracts major spectral components with the help of data-adaptive filters. This last has the advantage of allowing the identification of pseudo periodicities, with amplitudes that can vary on time, as most of the natural signals do. The method was implemented using the SSA-MTM toolkit of Dettinger et al. (1995) and Ghil et al. (2002).

4. Results and discussion

4.1. Suspended matter annual mean pattern and its forcings

The mean concentration of SM and its standard deviation estimated from the MODIS-Aqua observations computed over the 10-years analyzed period are shown in Fig. 4. The first feature that emerges is a change in the orientation of the mean concentration gradients at approximately Barra del Indio (Fig. 4a), which suggests a change of the dominant sedimentological processes upstream and downstream the shoal. Upstream the shoal, the SM concentration increases from northeast (with values less than 10 g m^{-3}) to southwest. The maximum extends along the southern coast of the estuary, from its head to Punta Piedras, with values more than 70 g m^{-3}. This maximum also broadens at the intermediate estuary, northwestward Punta Piedras. Seawards the shoal, instead, a marked offshore decay of the SM concentration is observed, with the gradient aligned with the estuary axis. High SM values are also observed along the coast of Samborombón Bay, with a relative maximum northward Punta Rasa. High variability (Fig. 4b) is observed in the entire upper and intermediate estuary, with a maximum over the Barra del Indio shoal, to the north of Punta Piedras, and decays offshore up to approximately a line between Punta Rasa and Punta del Este.

For comparison, the upper panel of Fig. 5 shows the mean concentration of surface SM and its standard deviation, computed from the *in-situ* water samples collected during the six cruises of the FREPLATA/FFEM Experiment. In spite of the large differences in the sources and amount of data used to build each figure, the correspondence between the maps derived from the remote

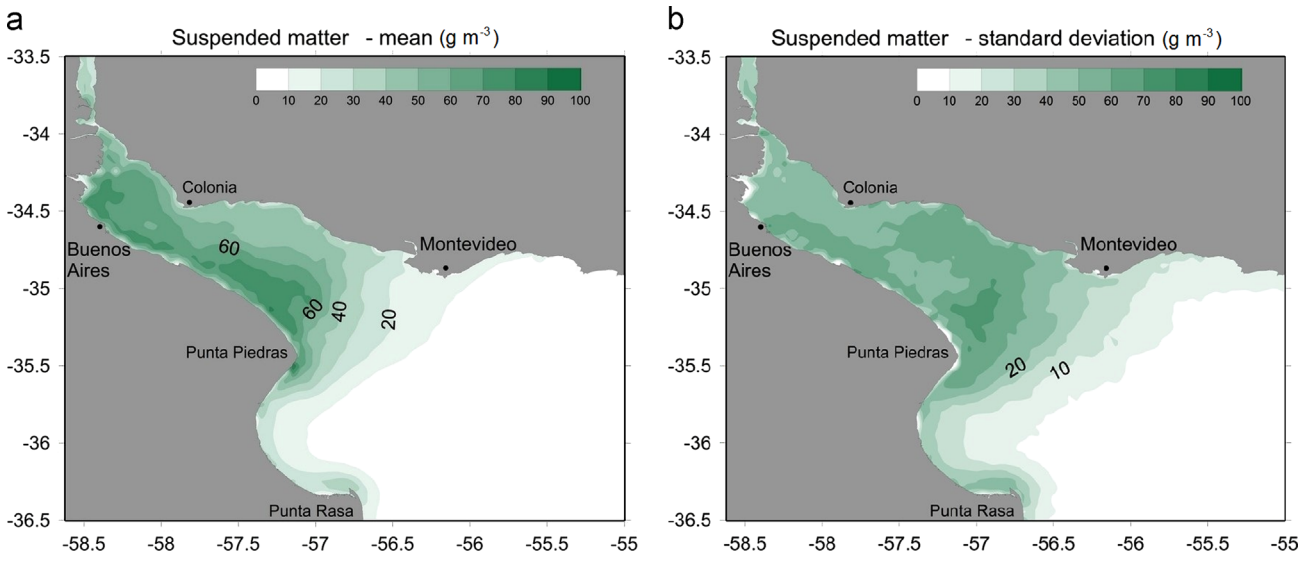

Fig. 4. Surface mean (a) and standard deviation (b) of the suspended matter concentration (g m^{-3}) computed from the MODIS-Aqua observations calibrated with the IFREMER algorithm for coastal turbid waters for the period 2002–2012.

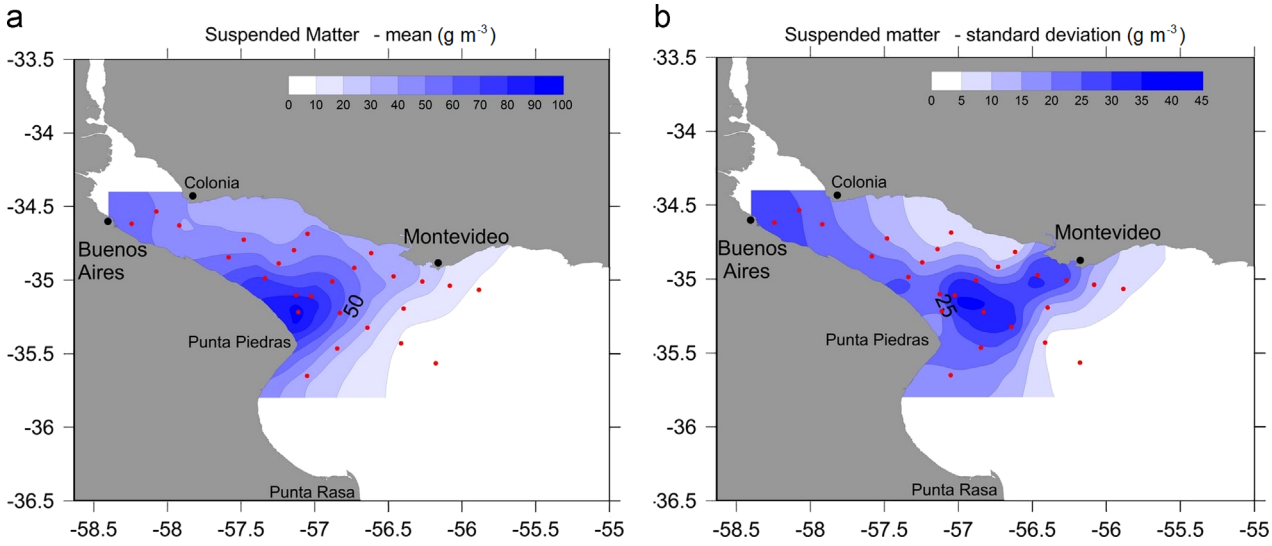

Fig. 5. Surface mean (a) and standard deviation (b) of the suspended matter concentration (g m^{-3}) derived from the water samples collected during the six cruises of the FREPLATA/FFEM Experiment. Dots indicate the sampling sites.

(Fig. 4a and b) and *in-situ* (Fig. 5a and b) observations is very good in what regards the magnitude and spatial distribution of both the mean surface SM concentration and its standard deviation (the typical error resulted of 11 g m^{-3}). Fig. 3b depicts a scatter plot of the *in-situ* SM concentration *vs.* the *in-situ* turbidity observed from the water samples collected during the six FREPLATA/FFEM Experiment cruises. This figure includes all the observations available, over the whole RDP. The correlation between variables is high (0.93) and seems to be linear everywhere, with no obvious change in the link among variables at different locations of the estuary. The empirical relationship between SM concentration and turbidity derived from these data is SM=0.73*turbidity. This relation displays great variability from one location to another depending – in part – of the nature, shape and size of the particles. For instance, Gohin (2011) finds a slope of 1.85 for the Dunkerque and Boulogne (southern North-Sea and eastern English Channel) areas and Snedden et al. (2007) report a slope of 0.89 for the Breton Sound estuary (Mississippi river), whereas Petus et al. (2010) estimate a value of 0.739 -similar to the one we find for the RDP- in the Basque coastal waters (Adour river).

The relatively larger SM concentrations observed along the southern coast of the upper and intermediate estuary (Figs. 4a and 5a) might be linked, at least in part, with the higher solid discharge of the Paraná River compared to the Uruguay River (Jaime and Menéndez, 2002). Solid discharge reaches the RDP mainly through the Paraná River (see Figs. 1 and 2), whereas the Uruguay River load is much smaller. The Paraná waters enter the estuary in two main branches: the Paraná de las Palmas, in the upper estuary close to Buenos Aires city, and the Paraná Guazú, further north close the Uruguay River mouth (Fig. 1). The second branch transports approximately 70% of the runoff of the Paraná River and, consequently, a proportional amount of solid materials (Bombardelli et al., 1995). Simionato et al. (2009) show that the plumes of the main tributaries to the estuary tend to keep approximately separated during their path along the upper and intermediate RDP. The waters of the Paraná Guazú and Paraná de

las Palmas tend to occupy the central and southern portion of the channel, respectively, whereas the Uruguay River waters are limited to the north. This can explain why the concentration of surface SM is larger in the southern than in the northern portion of the upper and intermediate RDP, but does not account for the maximum observed along the Argentinean (southern) coast (Figs. 4a and 5a).

Notwithstanding, the tidal wave enters into the RDP from the southeast and freely propagates following the coast as a Kelvin wave forced at its mouth (O'Connor, 1991), leaving the coast to the left in the Southern Hemisphere and having maximum amplitudes along the southern coast of the estuary (Simionato et al., 2004a). As in the RDP dissipation by bottom friction is large, most of the energy is lost before the tidal wave reaches the upper estuary (Framiñan et al., 1999); as a consequence, tides have small amplitude in the upper estuary and along its northern coast. This way, tidal currents are also stronger along the Argentinean coast than along the Uruguayan one (Simionato et al., 2004a), and might be responsible for more re-suspension of sediments in the former, leading to the maximum SM observed in Figs. 4 and 5. In effect, note the marked correspondence of the regions with maximum SM concentration shown in Figs. 4a and 5a and the geographical distribution of the areas of largest tidal energy dissipation by bottom friction shown by Simionato et al. (2004a) in their Figure 14. Those areas do not only extend along the southern coast of the upper and intermediate RDP, but also maximum tidal currents occur close to Punta Piedras and Punta Rasa, which are regions where SM concentration also maximizes (Figs. 4 and 5).

The rapid offshore decay of the surface SM concentration that occurs just seawards the Barra del Indio shoal (Figs. 4a and 5a) must be related to a different mechanism. In this sense, the upper and lower panels of Fig. 6 show the mean surface and bottom turbidity and salinity, respectively, computed using the observations gathered with the CTD/OBS3+ during the six FREPLATA/FFEM experiment's cruises. Fig. 6a and b also reveal that in the upper and intermediate RDP both the mean surface and bottom turbidity increase southward; nevertheless bottom values are considerably larger everywhere. In the exterior estuary maximum bottom concentrations, with values up to 200 g m^{-3}, are observed seaward the Barra del Indio shoal, to the east the surface turbidity maximum. This last area is associated with the tip of the bottom salinity front (Fig. 6d) and is where the physicochemical flocculation processes are supposed to become important (Ayup, 1986, 1987; Simionato et al., 2011a, 2011b). Here, flocculation/deposition must dominate over re-suspension to drive the strong decay of the surface SM concentration and turbidity patterns observed

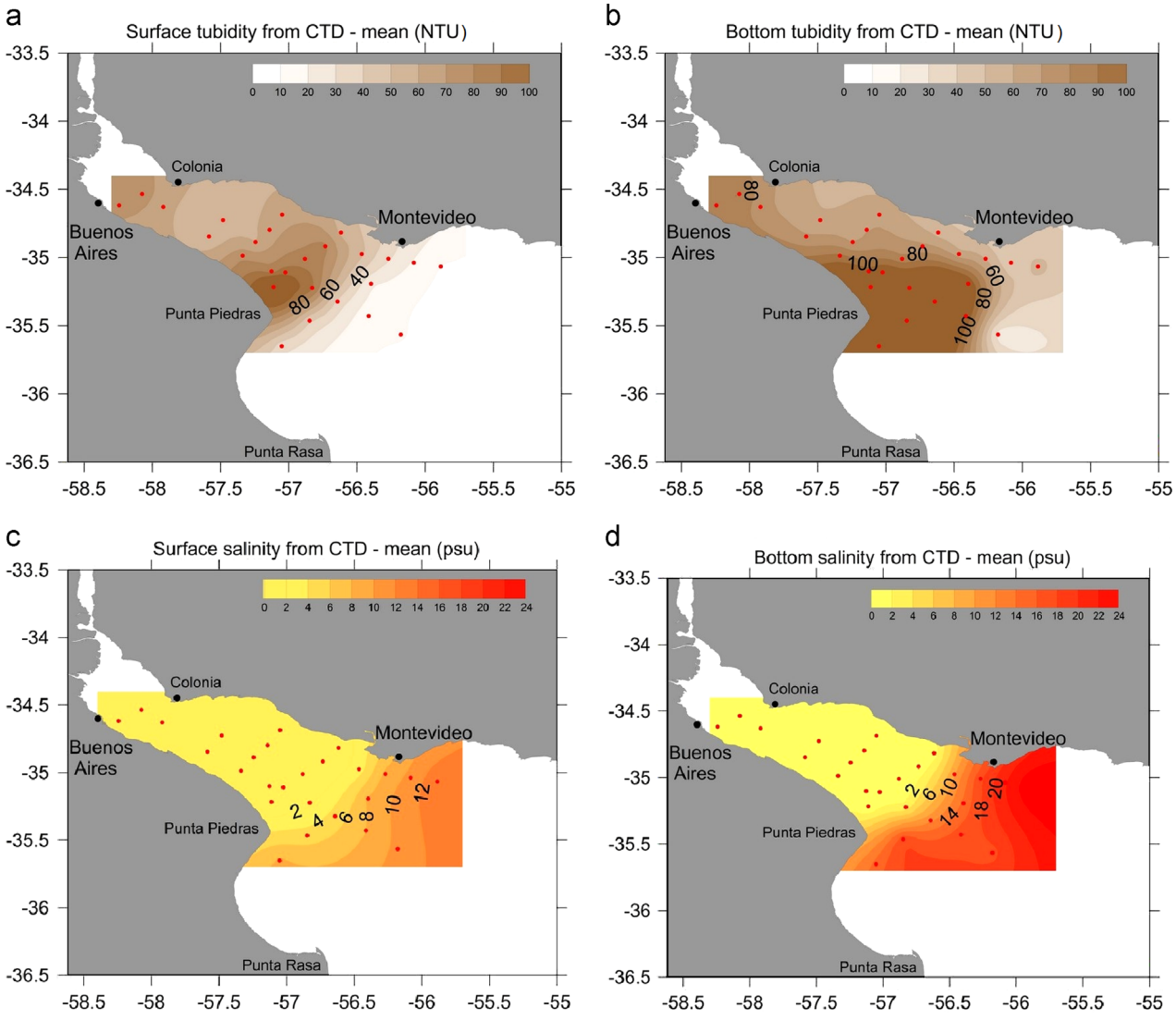

Fig. 6. Surface (left) and bottom (right) mean turbidity (upper panel, NTU) and salinity (lower panel, PSU) computed from the CTD/OBS observations collected during the six cruises of the FREPLATA/FFEM Experiment. Dots indicate the sampling sites.

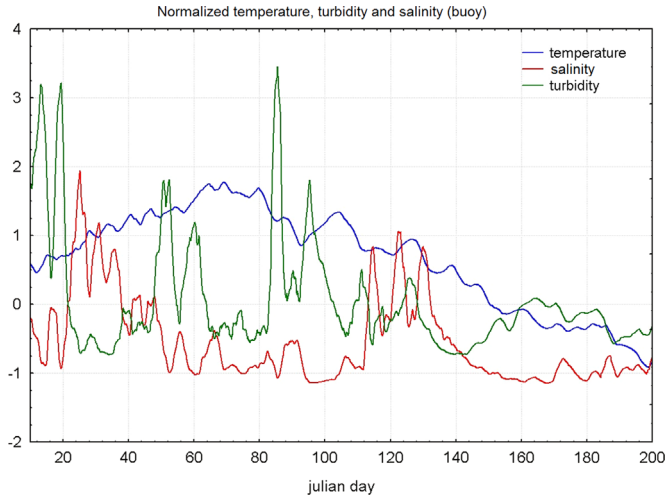

Fig. 7. Time series of the smoothed and normalized turbidity (green), temperature (blue) and salinity (red) for 200 days of the record gathered by the oceanographic buoy at Pontón Recalada. The observations span the period December, 2009–June, 2010. (For interpretation of the references to color in this figure legend, the reader is referred to the web version of this article.)

in Figs. 4–6. Another argument to explain this fact is related to the change in depth in the area. Seawards the Barra del Indio shoal, depth rapidly increases (Fig. 2), reducing the potential effect of wind waves on vertical mixing and re-suspension. Moreover, in the region of the salinity front bottom residual currents are also weak (Simionato et al., 2007).

Immediately offshore Barra del Indio, in addition, maximum surface SM variability is also observed (Figs. 4b and 5b). This area coincides with the maximum bottom and vertical salinity gradients (Fig. 6c and d), suggesting advective effects related to the RDP fresh water plume. The maximum standard deviation of the surface SM concentration observed in this area would be forced by the short time scale onshore–offshore motions of the fresh and turbid water plume forced by the winds. The data collected at Pontón Recalada during the FREPLATA/FFEM Experiment support this hypothesis. Fig. 7 shows the temporal evolution of the (normalized by the standard deviation) temperature, salinity and turbidity observed at that station for a period of 200 days between December, 2009 and June, 2010; a three days moving average filter was applied to the data. The figure illustrates the effect of the fresh plume advection on turbidity. In effect, high coherence between variables is evident at the atmospheric synoptic to intra-seasonal time scales. Note that increments in turbidity (and in temperature in a less extent, given that this variable is highly impacted by the seasonal cycle) are accompanied by reductions in salinity and *vice versa*.

4.2. *Seasonal cycle and its forcings*

Fig. 8 displays the mean surface SM concentration for every season of the year derived from the MODIS-Aqua observations, which suggests the occurrence of a seasonal cycle. In the upper and intermediate RDP, SM concentration increases in the austral fall and maximizes in winter, with mean values more than 80 g m^{-3} along the southern coast, and less than 60 g m^{-3} along the northern coast. The minimum occurs in summer, when values along the northern coast reduce to less than 20 g m^{-3}. The *in-situ* observations gathered during the six FREPLATA/FFEM Experiment's cruises support the occurrence of such a seasonal cycle in surface SM/turbidity concentration (Fig. 9). Even though the SM concentration spatial distribution showed large temporal variability from one to other cruise (see the large standard deviation in Figs. 4b and 5b), they indicate a general trend to lower concentrations in spring-summer than in fall-winter. As an example, Fig. 9 displays the surface SM observed during the cruises made in June and December, 2010. Note the overall lower SM observed in the area of study during December (austral summer) than during June (austral winter). In the outer RDP a significant variation of the SM concentration occurs from the warm to the cold seasons, particularly along the northern coast of the estuary, around Montevideo (see Fig. 8). As we will discuss later, it could be due to a different forcing mechanism.

To better study the seasonal cycle and its driving processes, we calculated the spatial average of the surface SM concentration daily values derived from MODIS-Aqua data for the five different regions of the RDP shown as red squares in Fig. 8b, which represent areas that in principle would be related to diverse dynamics:

- Region 1: upper RDP.
- Region 2: intermediate RDP.
- Region 3: bottom salinity front.
- Region 4: Samborombón Bay.
- Region 5: Uruguayan coast.

Results are shown in Fig. 10a–e, where the black lines display the mean daily values, whereas the red lines represent 30 days moving averages. Fig. 11 displays, overlapped, the mean annual cycle computed for regions 2, 4 and 5; results for regions 1 and 3 resulted very similar than for region 2 and, therefore, are not shown. The ± 1 standard deviation lines have been also included (dotted lines) to provide information about the data dispersion. Figs. 10 and 11 indicate that the seasonal cycle is a robust signal in the entire RDP, excepting along the Uruguayan coast of the outer estuary, where it is much weaker. Along that coast, Fig. 8 suggests that the surface SM seasonal cycle would be linked to the seasonal displacement of the RDP fresh water plume, which more often advects fresh water (and sediments and nutrients) to the northeast, or the Uruguayan coast, in fall-winter and to the southwest, or Argentinean coast, in spring-summer (Guerrero et al., 1997; Simionato et al., 2001; Simionato et al., 2007).

In what regards the seasonal signal observed in the upper and intermediate estuary (Figs. 10a, b, c and 11), SM concentrations are small between December and February, begin to grow in March, maintain high during the austral fall and winter, and reach a maximum in August (end of the austral winter). After that month they monotonically decay up to December. This seasonal cycle could be forced by either the seasonality of the solid discharge or the winds, or both.

The mean annual cycle of the solid discharge of the Bermejo River (the main source of sediments to the estuary) is shown as a solid black line overlapped in Fig. 11. It is low between May and November, begins to grow in December and reaches its maximum between March and April. The travel time of the water and sediments load from El Colorado station (where the load has been measured) to the RDP estuary head can be estimated in 13 days, considering a mean water speed of 1 m s^{-1}. Guerrero et al. (2004) estimated the travel time of the waters of the estuary from its head to the bottom salinity front in 22 days for mean runoff conditions, and varying between 19 and 32 days for high and low water discharge conditions, respectively. Simionato et al. (2009) made estimations using a numerical model, with quantitatively similar results. This way, the total travel time of the waters and sediments of Bermejo River from El Colorado to the mixing zone of the RDP can be estimated of the order of one month for mean runoff conditions. In this sense, if the SM concentration in the RDP were only modulated by the solid runoff to the estuary, one would expect a maximum in April, followed by high values in May, and a rapid decay during the next months. Figs. 10 and 11 show that,

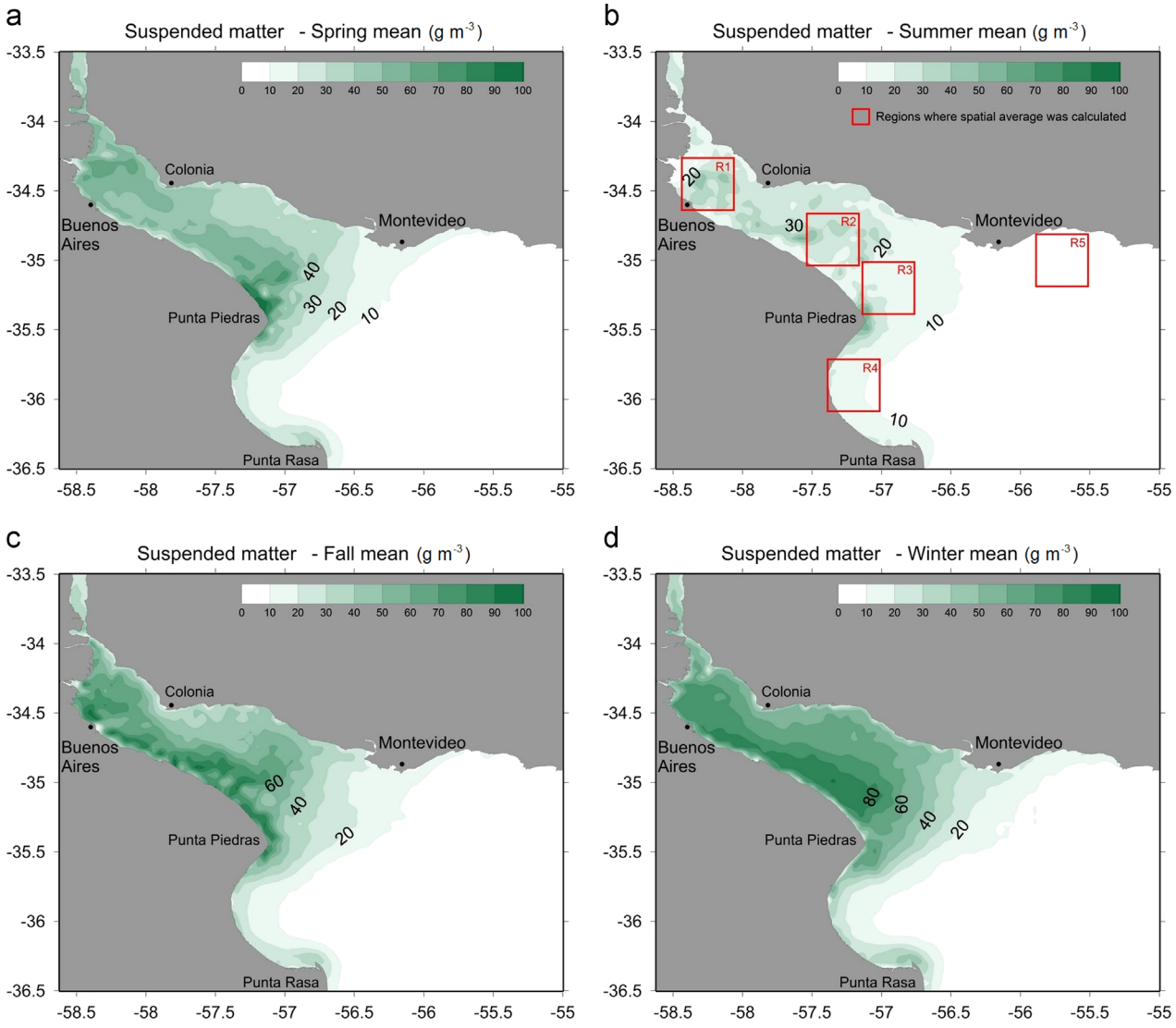

Fig. 8. Mean suspended matter concentration (g m^{-3}) computed from the MODIS-Aqua observations for the period 2002–2012 calibrated with the OC5 algorithm for turbid coastal waters for (a) spring, September–November; (b) summer, December–February; (c) fall, March–May; (d) winter, June–August.

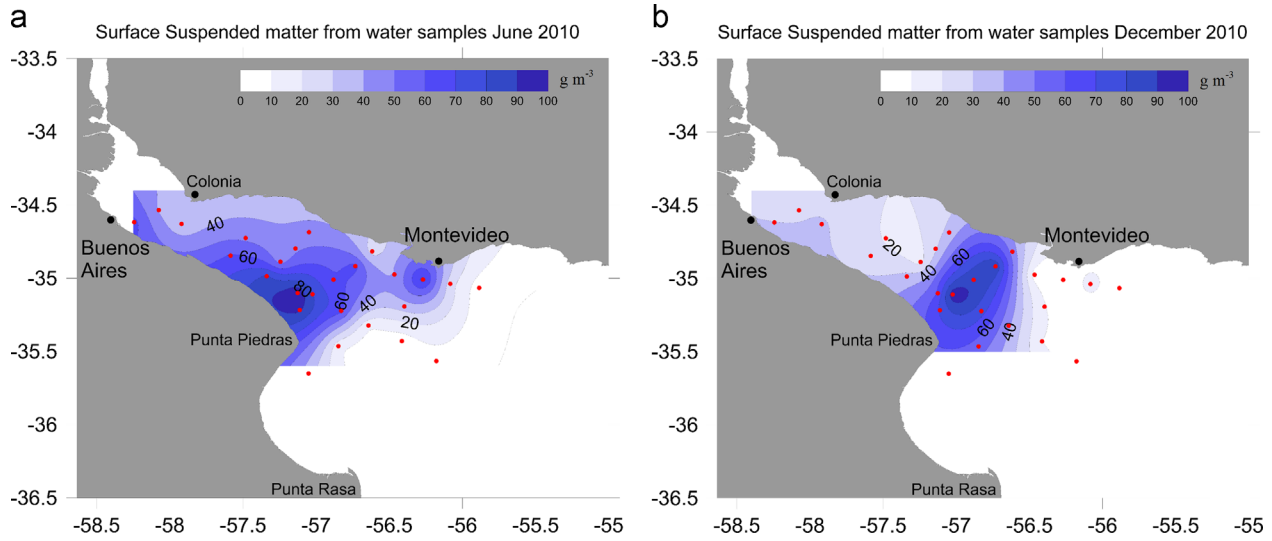

Fig. 9. Surface SM concentration (g m^{-3}) derived from the water samples collected during the cruises made in June (a) and December (b) 2010.

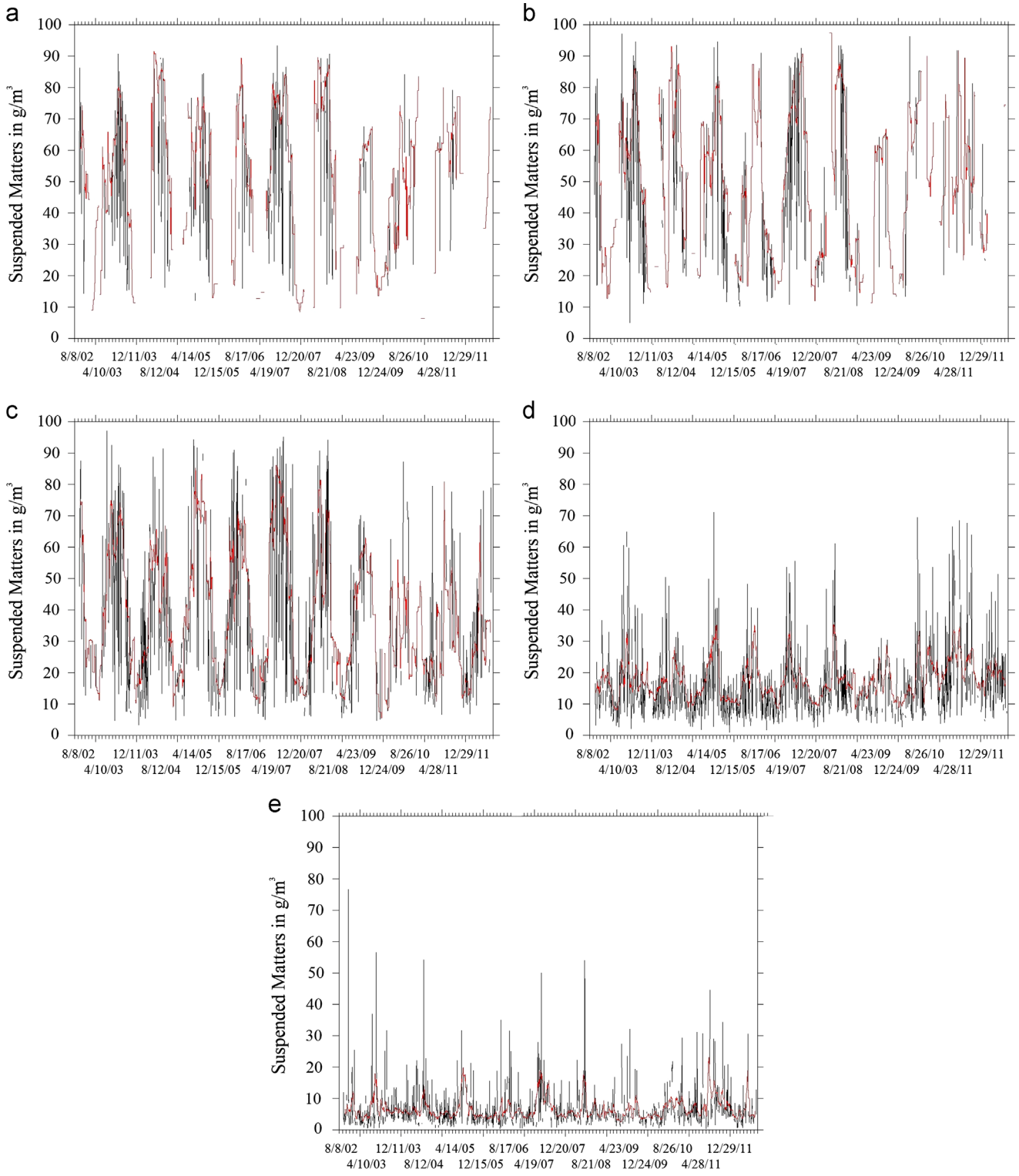

Fig. 10. Time series of the spatial mean SM concentration (g m^{-3}) computed for the five regions identified as red squares in Fig. 8b; the black lines display the mean daily values, whereas the red lines represent 30 days moving averages. (For interpretation of the references to color in this figure legend, the reader is referred to the web version of this article.) (a) Upper RIo de la Plata, (b) intermediate RIo de la Plata, (c) bottom salinity front, (d) samborombon bay and (e) uruguayan coast.

in effect, a rapid increase of the SM concentration occurs in April; nevertheless values maintain high during the entire fall and winter, reaching a maximum at the end of this last season which cannot be accounted by the solid runoff. The liquid runoff can neither account for a winter maximum in the SM concentration, given that it maximizes during that season (Nagy et al., 1997), driving in any case to a larger dilution.

A possible mechanism for the winter maximum observed in the surface SM concentration in Figs. 8–11 is re-suspension and vertical mixing by wind waves. As above mentioned, winds in the area are characterized by an alternation from northeasterlies, due to the quasi-permanent South Atlantic High, to southwesterlies, due to the impact of frontal systems over the area, with a characteristic period of around 4 days. In the RDP the number of

fronts reaching the region from the south grows in winter, tending to increase the number of strong wind events. In summer, winds from the north and northeast directions of moderate speed dominate; in winter, instead, strong winds from the southwest become more frequent (Simionato et al., 2005a). This last would increase the number of events with both stronger currents and wind waves in the RDP during that season, driving to a larger number of re-suspension events during the cold period. In addition, under strong and/or persistent westerly/southwesterly winds, the RDP water level tends to reduce (Simionato et al., 2004b; Campetella et al., 2007); this would be, in turn, favorable to re-suspension and vertical mixing and, therefore, to higher surface SM concentrations. Unfortunately, there are not long term observations of wind waves in the upper and intermediate RDP to verify that hypothesis with a climatology, but simultaneous wind, wind waves and turbidity observations were collected at the oceanographic buoy and Pilote Norden and Torre Oyarvide during a few months during the FREPLATA/FFEM Experiment. Those data are presented in Fig. 12, showing a clear connection between stronger winds, higher waves and increased turbidity, which supports our hypothesis.

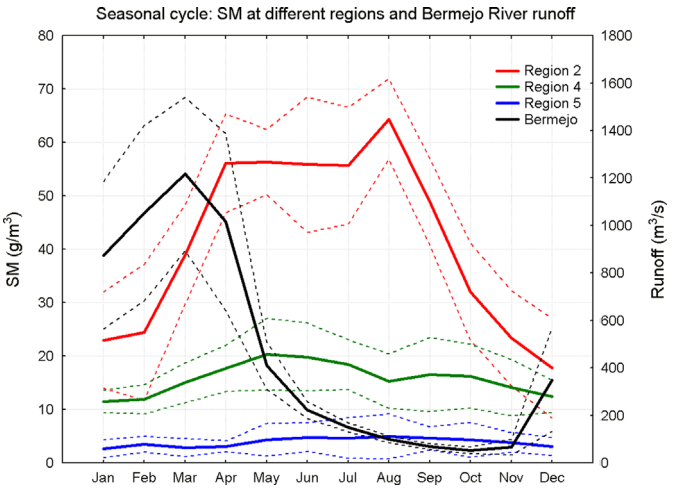

Fig. 11. Mean annual cycle of the SM concentration (g m^{-3}) computed for regions 2, 4 and 5, red, green and blue solid lines, respectively. The ± 1 standard deviation limits are shown as dotted lines in the same colors. Superimposed, the black lines show the solid discharge of the Bermejo River and its ± 1 standard deviation limits. (For interpretation of the references to color in this figure legend, the reader is referred to the web version of this article.)

To further analyze the above mentioned connection, a multi channel singular spectral analysis (MSSA) was applied to the normalized series of the wind burst measured at Pontón Recalada and the wave height and turbidity gathered at Torre Oyarvide between October 26th and December 17th, 2010 (53 days). Wind burst was selected as the analyzed variable instead of wind speed because it is more representative of the storm events and therefore, of wave generation; nevertheless, it was verified that results do not change significantly if the wind speed is used instead. To evaluate the impact of tides on turbidity, the astronomic tide was added to the analysis. Results show that the series have common periodicities at periods around 12.5 h (20.4% of the total variance), 8.5 days (12.3% of the variance), 4.5 days (8.4% of the variance) and 24 h (3.6% of the variance). Note that whereas 12.5 and 24 h are associated tides and sea breeze, 8.5 and 4.5 days are periods which are connected to the characteristic synoptic atmospheric variability in the area (Vera et al., 2002). Fig. 13 shows the reconstructed components of each of the analyzed series for those periods. The reconstruction of the pseudo periodicities centered at 8.5 and 4.5 days (Fig. 13b and c) show that waves and turbidity respond to wind variability on those time scales. An increase (decrease) of the wind and its burst is accompanied by a simultaneous increase (decrease) of the wave height, and with an increase (decrease) of the turbidity a few hours later, supporting our hypothesis

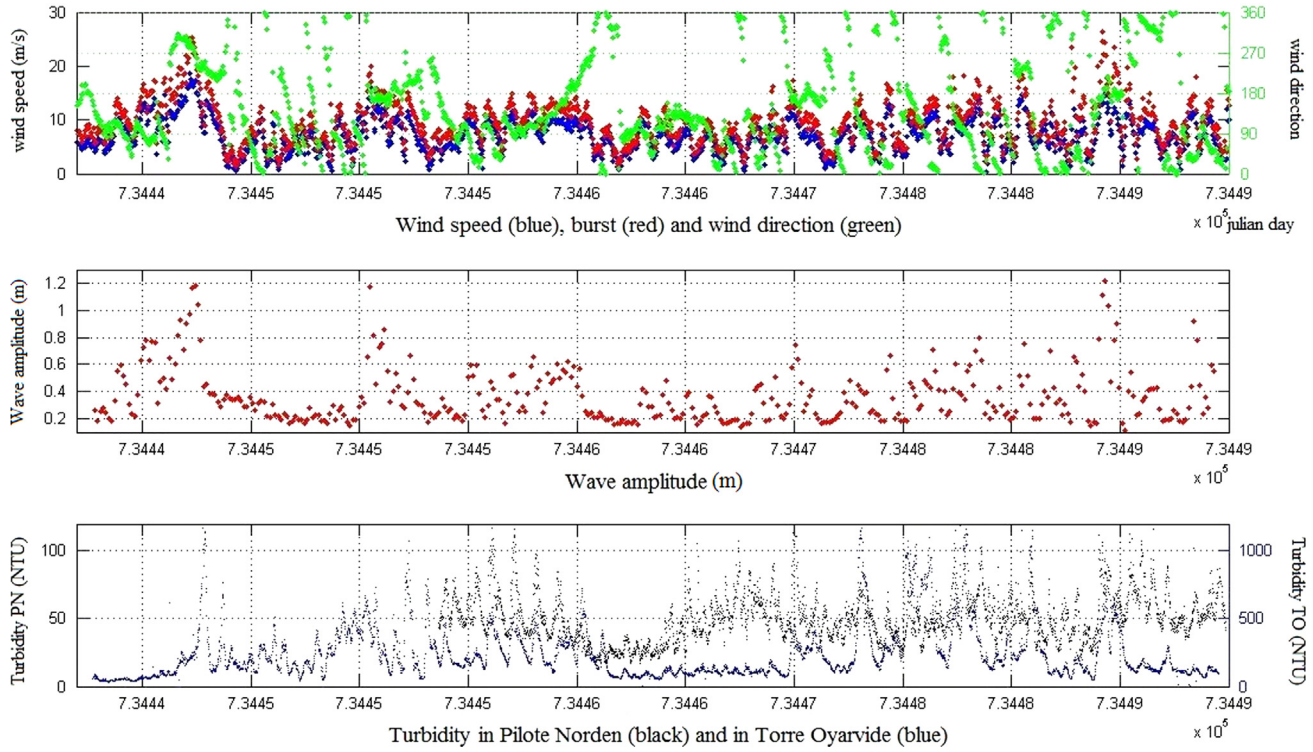

Fig. 12. (a) Hourly wind speed (blue, m s^{-1}), burst (red, m s^{-1}) and direction (green, deg) recorded at Pontón Recalada by the oceanographic buoy; (b) wave amplitude (m) recorded every 15 min in Torre Oyarvide and (c) turbidity (NTU) recorded every 15 min in Pilote Norden (black) and Torre Oyarvide (blue). The plots correspond to the period October to December, 2010. (For interpretation of the references to color in this figure legend, the reader is referred to the web version of this article.).

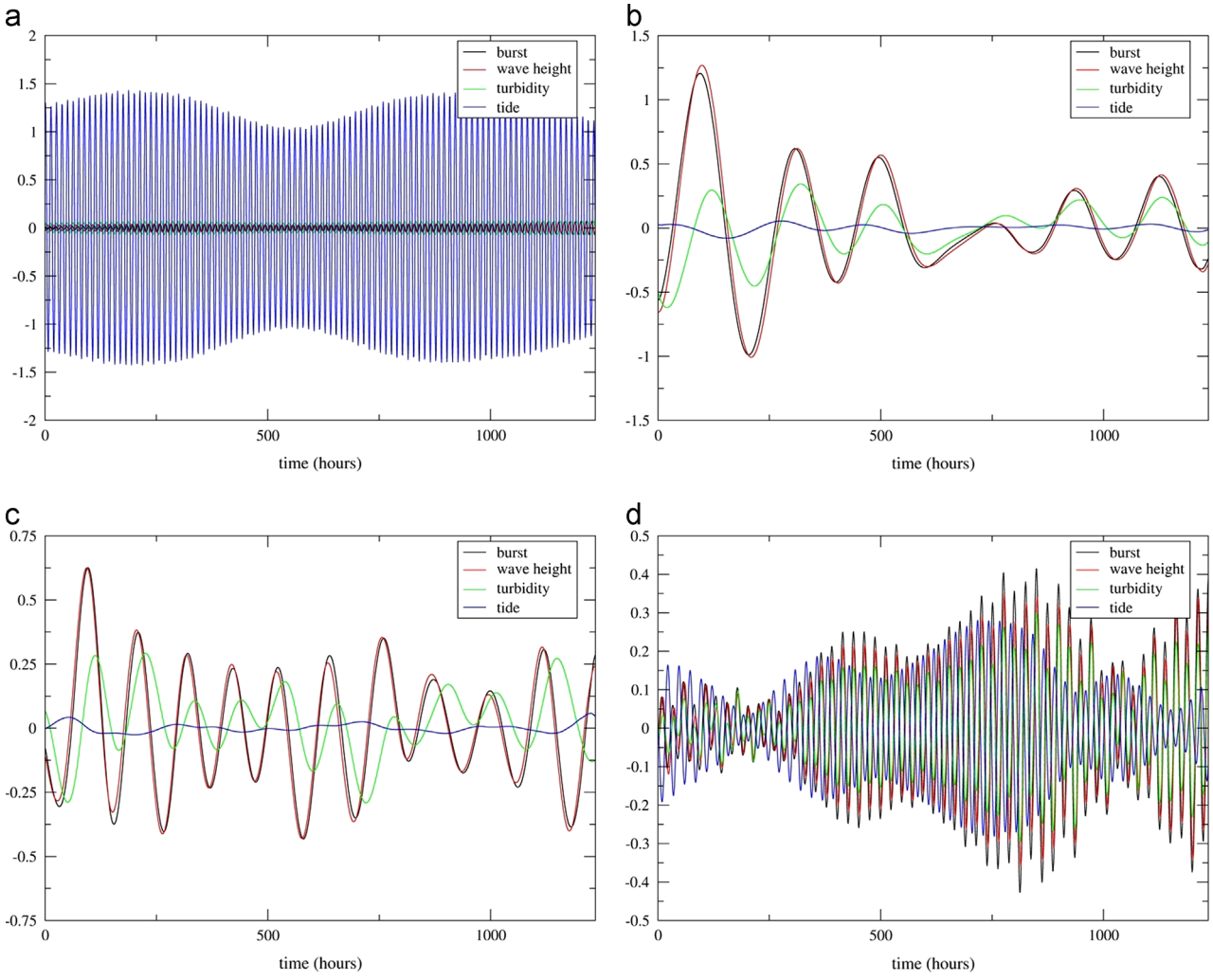

Fig. 13. Reconstruction of the pseudo periodicities in wind burst (black), wave height (red), turbidity (green) and tides (blue) identified by means of MSSA at periods centered at (a) 12.5 h, (b) 8.5 days, (c) 4.5 days and (d) 24 h. All the variables have been normalized previous to the analysis. (For interpretation of the references to color in this figure legend, the reader is referred to the web version of this article.).

that wind waves play a central role in the determination of surface turbidity in this region. Periodicities at 24 h (Fig. 13d) seem to be related to sea breeze more than to tides, as the amplitude is not modulated by the spring-neap tide cycle, but seems to become more important when synoptic variability decays (compare Fig. 13 b and c). The impact of sea breeze on currents in this area has been reported by Simionato et al. (2005b), who showed that they can be responsible for as much variance as the barotropic tides. Stronger (weaker) winds are again followed by an increment (reduction) in the wind waves height and turbidity. The statistical methodology projects part of the tidal variance in this period on the reconstruction, with an increment (reduction) of the sea level associated with a reduction (increment) of the turbidity. Finally, the reconstruction of the periodicities in 12.5 h (Fig. 13a), clearly due to tides and modulated by the spring-neap tidal cycle, reveals that at Torre Oyarvide tides have a small direct impact on surface turbidity. Note, nevertheless, that Torre Oyarvide is located in the area where the maximum surface SM is observed (Figs. 4 and 5), and that we connected to tides in the previous section. This apparent contradiction can be probably explained by the fact that tide acts mainly on the bottom, re-suspending sediments on the lower part of the column and making them available. Then, winds and the forced waves can act vertically, mixing the column and modifying the surface properties. In this sense a similar analysis (not shown) was applied to the wind burst measured at Pontón Recalada and the wave height, turbidity and tides observed at Pilote Norden. In this case, the available series are too short to properly reveal variability in the atmospheric synoptic time scale. Nevertheless in this site, located in a shallower region than Torre Oyarvide, tides seem to directly play a more important role on determining surface turbidity, accounting for a larger percentage of the variance.

5. Summary of conclusions

In this paper we analyze SM observations in the RDP estuary with the aim of characterizing the annual mean values and the seasonal cycle and to identify the involved physical mechanisms. We used *in-situ* data collected during the FREPLATA/FFEM Experiment. It included six oceanographic cruises performed every approximately two months, between November, 2009 and December, 2010, which provided quasi synoptic fields and profiles of salinity, temperature and turbidity in the entire estuary. During the cruises, water samples were also collected, which were analyzed for SM concentration and turbidity. Additionally, we used time series gathered at three fixed points of the RDP, providing high temporal resolution observations of waves, winds and turbidity. We complement the study with ten years of 1 km-resolution MODIS-Aqua ocean color observations in the RDP and the adjacent shelf, processed for surface SM concentration with the IFREMER algorithm for coastal turbid waters.

The simultaneous use of *in-situ* and remote observations has allowed, for the first time, a robust characterization of the mean distribution pattern of the SM concentration and turbidity in the RDP and its variability on seasonal time scales, so as the identification of the most likely driving processes. The mean surface SM concentration inferred from the color remote observations using the IFREMER algorithm and their variability well compare with those derived from the *in-situ* observations. There is a good correspondence in the magnitude and the spatial distribution of the maxima, minima and gradients. A marked resemblance is observed between the spatial patterns of the surface SM concentration and turbidity. A linear link between both variables is observed over the whole estuary, without apparent spatial differences.

Our principal results can be summarized as follows:

- In the upper and intermediate estuary the spatial pattern of the mean surface SM concentration is mainly controlled by both the solid discharge and the re-suspension by tides. As both, the tributaries' solid discharge and tidal currents are larger to the south, the mean surface SM concentration maximizes along that coast all along the year. Maximum concentrations are observed close to Punta Piedras and seem to be highly correlated with the one of the areas of maximum tidal currents and tidal dissipation by bottom friction of the estuary shown by Simionato et al. (2004a). Our results suggest that tides act re-suspending the sediments near the bottom, but wind waves vertically mix the water column making the sediments reach the surface.
- In the outer RDP the mean surface SM concentration decays seawards, but displays maximum temporal variability and horizontal gradients. This area coincides with the tip of the bottom salinity front and the region were both the horizontal and vertical salinity gradients are maxima. Here the leading processes would be flocculation and decantation and the wind-forced fresh water plume dynamics. Tides and waves act re-suspending sediments and mixing, but play a secondary role, because depth here is larger.
- There is a secondary maximum of the mean surface SM concentration in the outer estuary, close to Punta Rasa, which seems to be connected to another area of maximum tidal currents and tidal dissipation by bottom friction. In this area wave action becomes more important, as the depth decreases.
- Surface SM concentration displays a marked seasonal cycle with maximum values in the austral fall-winter and minimum values in summer in most of the estuary, excepting the Uruguayan coast around Montevideo. The rapid increase observed in the SM concentration during March and April seems to be related with the seasonal cycle of the main solid discharge tributary to the estuary, the Bermejo River, which occurs in February and March. Nevertheless, SM concentration maintains high in the entire estuary up to September and maximizes in August (end of the austral winter). This maximum would be forced by the higher frequency of storms, inducing stronger southwesterly winds, during that season. They would produce an increase in the frequency of higher waves, which could cause further re-suspension and/or vertical mixing.
- Along the Uruguayan coast and the exterior RDP, close to Montevideo, a weaker seasonal signal with a relative minimum in summer and a maximum in winter is observed. This cycle would be linked to the seasonal displacement of the RDP fresh water plume, which more often advects fresh water (and presumably sediments and nutrients) to the northeast, or the Uruguayan coast, in winter and to the southwest, or Argentinean coast, in summer.

Our conclusions do not only contribute to a better understanding of the sedimentological processes in this important estuary, but will also help on the construction and validation of numerical models, which are needed for management and scientific purposes. Those studies, including future biogeochemical modeling are envisaged as a continuation of this research.

It is important to note that further development of the algorithms used to calibrate the MODIS-Aqua color observations is needed for the RDP, particularly over its most turbid areas. In this sense, the collection of radiometric samples (not available yet) together with *in-situ* observation of turbidity, SM and Chl-*a* and bio-optical properties is fundamental. Efforts to progress in this direction are being made by the working group.

Acknowledgments

This study was funded by the FFEM (Fonds Français pour l'Environnement Mondial of France) in the frame of the PNUD/GEF RLA/99/G31 FREPLATA Project, the ANPCyT (National Agency for Scientific and Technological Research of Argentina) PICT 2010-1831 and the CONICET (National Council for Scientific and Technological Research of Argentina) PIP 112 201101 00176 Projects. Diego Moreira's and Moira Luz Clara's participation were also allowed by UBA and CONICET Ph.D. fellowships, respectively.

References

Acha, M.E., Mianzan, H., Lasta, C.A., Guerrero, R.A., 1999. Estuarine spawning of the whitemouth croaker Micropogonias furnieri (Pisces: Sciaenidae), in the Río de la Plata, Argentina. Marine and Freshwater Research 50 (1), 57–65.

Acha, E.M., Macchi, G.J., 2000. Spawning of Brazilian menhaden, Brevoortia aurea, in the Río de la Plata estuary off Argentina and Uruguay. Fishery Bulletin (Washington, DC) 98, 227–235.

Acha, E.M., Simionato, C.G., Carozza, C., Mianzan, H., 2012. Climate induced year classes' fluctuations of whitemouth croaker Micropogonias Funieri (Pisces, Sciaenidae) in the Río de La Plata estuary, Argentina-Uruguay. Fisheries Oceanography 21 (1), 58–77, http://dx.doi.org/10.1111/j.1365-2419.2011.00609.x.

Ayup, R.N., 1986. Comportamento dos sedimentos em suspensao no Río de la Plata exterior e proximidades. Pesquisas 18, 39–68.

Ayup, R.N., 1987. Intercambio sedimentar entre o Río de la Plata Exterior e a plataforma continental adjacente. Pesquisas 19, 106–206.

Balay, M.A., 1961. El Río de la Plata entre la atmósfera y el mar. Publicación. H-621. Buenos Aires: Servicio de Hidrografía Naval. Armada Argentina. 153 pp.

Berasategui, A.D., Acha, E.M., Fernandez Araoz, N.C., 2004. Spatial patterns of ichthyoplankton assemblages in the Río de la Plata Estuary (Argentina-Uruguay). Estuarine, Coastal and Shelf Science 60, 599–610.

Berasategui, A.D., Menu Marque, S., Gómez-Erache, M., Ramírez, F.C., Mianzan, H.W., Acha, E.M., 2006. Copepod assemblages in a highly complex hydrographic region. Estuarine, Coastal and Shelf Science 66, 483–492.

Bombardelli, F., Menéndez, A., Lapetina, M., Montalvo, J., 1995. Estudio del impacto hidráulico del puente Buenos Aires-Colonia: informe No 1, Ezeiza, LHA, 1995, LHA-141-01-95, 25 pp.

Boschi, E.E., 1988. El ecosistema estuarial del Río de la Plata (Argentina y Uruguay). Anales del Instituto de Ciencias del Mar y Limnología, Universidad Nacional Autónoma de México, 15, pp. 159–182.

Bowers, D.G., Boudjelas, S., Harker, G.E.L., 1998. The distribution of fine suspended sediments in the surface waters of the Irish Sea and its relation to tidal stirring. International Journal of Remote Sensing 19 (14), 2789–2805.

Campetella, C.M., D'onofrio, E., Cerne, S.B., Fiore, M.M.E., Possia, N.E., 2007. Negative storm surges in the Port of Buenos Aires. International Journal of Climatology 27 (8), 1091–1101.

Campos, J.D., Lentini, C.A., Miller, J.L., Piola, R.A., 1999. Inter-annual variability of the sea surface temperature in the South Brazilian Bight. Geophysical Research Letters 26 (14), 2061–2064.

Canevari, P., Blanco, D., Bucher, E., Castro, G., Davidson, I., 1998. Los Humedales de la Argentina. Clasificación, Situación Actual, Conservación y Legislación. Publicado por Wetlands Internacional y Secretaría de Recursos Naturales y Desarrollo Sustentable de la Nación. Publicación No 46. Buenos Aires.

Cardini, J.C., Garea, M., Campos, M.R., 2002. Modelación del transporte de sedimentos puestos en suspensión por actividades de dragado en el Río de la Plata, para la generación en tiempo real de pronósticos de afectación de áreas costeras. Anales del Congreso de Mecánica Computacional, Santa Fé-Paraná, Argentina, Octubre de 2002. Publicado por Mecánica Computacional, 21, pp. 2325–2342.

Cavallotto, J.L., 1987. Dispersión, transporte, erosión y acumulación de sedimentos en el Río de la Plata. Informe final de Beca de Iniciación, Comisión de Investigaciones Científicas, La Plata – Argentina.
Cavallotto, J.L., Violante, R., 2008. Atlas Ambiental de Buenos Aires, ⟨http://www.atlasdebuenosaires.gov.ar⟩.
Codignotto, J.O., Dragani, W.C., Martin, P.B., Simionato, C.G., Medina, R.A., Alonso, G., 2012. Wind wave climate change and increasing erosion observed in the Río de la Plata, Argentina. Continental Shelf Research 38, 110–116 http://dx.doi.org/10.1016/j.csr.2012.03.013.
Colombo, J.C., Cappelletti, N., Barreda, A., Migoya, M.C., Skorupka, C., 2005. Vertical fluxes and accumulation of PCBs in coastal sediments of the Río de la Plata estuary, Argentina. Chemosphere 61 (9), 1345–1357.
Colombo, J.C., Cappelletti, N., Migoya, M.C., Speranza, E., 2007. Bioaccumulation of anthropogenic contaminants by detritivorous fish in the Río de la Plata estuary: 2-Polychlorinated biphenyls. Chemosphere 69 (8), 1253–1260.
Comisión Administradora del Río de la Plata (CARP), 1989. Estudio para la evaluación de la contaminación en el Río de la Plata, Report, Informe de la Comisión Administradora del Río de la Plata, Buenos Aires, 137 pp.
Cousseau, M.B., 1985. Los peces del Río de la Plata y su Frente Marítimo. In: Yañez-Arancibia, A. (Ed.), Fish Community Ecology in Estuaries and Coastal Lagoons: Towards an Ecosystem Integration. UNAM Press Mexico, pp. 515–534.
Depetris, P.J., Griffin, J.J., 1968. Suspended load in the Río de la Plata drainage basin. Sedimentology 11, 53–60.
Dettinger, M., Ghil, M., Strong, C.M., Weibel, C.M., Yiou, P., 1995. Software spedites singular-spectrum analysis of noisy time series. Eos, Transactions American Geophysical Union 76 (12), 14–21.
Dogliotti, A.I., Ruddick, K., Nechad, B., Lasta, C., Mercado, A., Hozbor, C., Guerrero, R., Riviello López, G., Abelando, M., 2011. Calibration and validation of an algorithm for remote sensing of turbidity over La Plata River estuary, Argentina. EARSeL eProceedings 10 (2), 119–130.
D'Onofrio, E., Fiore, M.M.E., Romero, S., 1999. Return periods of extreme water levels estimated for some vulnerable areas of Buenos Aires. Continental Shelf Research 19, 1681–1693.
Dragani, W.C., Codignotto, J.O., Martin, P.B., Campos, M.I., Alonso, G., Simionato, C.G., Medina, R.A., 2012. Some coastal impacts related to wind wave changes in south-eastern South American Continental Shelf. In: Proceedings of the Southern Ocean Oceanography, Climatic Impact. ISBN: 978-1-61470-462-1. Nova Science Publishers, Inc. 400 Oser Avenue, Suite 1600 Hauppauge, NY 11788, pp. 161–177.
Framiñan, M.B., Brown, O.B., 1996. Study of the Río de la Plata turbidity front: I. Spatial and temporal distribution. Continental Shelf Research 16, 1259–1282.
Framiñan, M.B., Etala, M.P., Acha, M.E., Guerrero, R.A., Lasta, C.A., Brown, O.B., 1999. Physical characteristics and processes of the Río de la Plata Estuary. In: Perillo, G.M., Piccolo, M.C., Pino Quivira, M. (Eds.), Estuaries of South America: Their Morphology and Dynamics. Springer, New York, pp. 161–194.
Ghil, M., Allen, M.R., Dettinger, M.D., Ide, K., Kondrashov, D., Mann, M.E., Robertson, A.W., Saunders, A., Tian, Y., Varadi, F., Yiou, P., 2002. Advance spectral methods for climatic time series. Reviews of Geophysics 40 (1), 1–41.
Glorioso, P.D., Flather, R.A., 1995. A barotropic model of the currents off SE South America. Journal of Geophysical Research 100, 13427–13440.
Glorioso, P.D., Flather, R.A., 1997. The Patagonian Shelf tides. Progress in Oceanography 40, 263–283.
Gohin, F., Druon, J.N., Lampert, L., 2002. A five channel chlorophyll algorithm applied to SeaWiFS data processed by SeaDAS in coastal waters. International Journal of Remote Sensing 23 (8), 1639–1661.
Gohin, F., Loyer, S., Lunven, M., Labry, C., Froidefond, J.M., Delmas, D., Huret, M., Herbland, A., 2005. Satellite-derived parameters for biological modelling in coastal waters: illustration over the eastern continental shelf of the Bay of Biscay. Remote Sensing of Environment 95 (1), 29–46.
Gohin, F., 2011. Annual cycles of chlorophyll-a, non-algal suspended particulate matter, and turbidity observed from space and *in-situ* in coastal waters. Ocean Science 7, 705–732, http://dx.doi.org/10.5194/os-7-705-2011.
Gómez-Erache, M., 1999. Spatial and temporal variation in the copepod community of Montevideo Bay, Uruguay. In: Proceedings of the World Association of Copepodologists: Seventh International Conference on Copepoda, Curitiba, pp. 25–31; Program and Abstracts: 121. (Abstract; 25.vii.1999).
Gómez-Erache, M., Sans, K., Danilo, C., Menu Marque, S., 2004. Recent data on freshwater Cyclopoid Copepoda (Cyclopoida: Cyclopidae) from Uruguay. Nauplius 11 (2), 145–148.
Guarga, R., Vinzón, S., Rodríguez, H., Piedra-Cueva, I., Kaplan, E., 1991. Corrientes y sedimentos en el Río de la Plata, Informe Técnico del IMFIA, Montevideo, Uruguay.
Guerrero, R.A., Acha, E.M., Framiñan, M.B., Lasta, C.A., 1997. Physical oceanography of the Río de la Plata Estuary, Argentina. Continental Shelf Research 17 (7), 727–742.
Guerrero, R.A., Molinari, G., Jauregui, S., 2004. Datos meteorológicos y climatología. Informe Final. Informe FREPLATA INIDEP A5 (21), 13 ⟨http://www.freplata.org⟩.
Huret, M., Dadou, I., Dumas, F., Lazure, P., Garçona, V., 2005. Coupling physical and biogeochemical processes in the Río de la Plata plume. Continental Shelf Research 25 (5–6), 629–653.
Instituto Nacional del Agua (INA), 2010. Generación y transporte de sedimentos en la Cuenca Binacional del Río Bermejo. Caracterización y análisis de los procesos intervinientes. 1a ed. Buenos Aires. ISBN 978-987-25793-7-1, COBINABE, 2010, 230 p.
Jaime, P.R., Menéndez, A.N., 2002. Análisis del régimen hidrológico de los ríos Paraná y Uruguay, informe LHA-01-216-02, INA, Ezeiza.
Jaureguizar, A., Bava, J., Carozza, C., Lasta, C., 2003a. Distribution of the whitemouth croaker (*Micropogonias Furnieri*) in relation to environmental factors at the Río de la Plata Estuary, South America. Marine Ecology Progress Series 255, 271–282.
Jaureguizar, A., Menni, R., Bremec, C., Mianzan, H., Lasta, C., 2003b. Fish assemblage and environmental patterns in the Río de la Plata estuary. Estuarine, Coastal and Shelf Science 56 (5–6), 921–933.
Jaureguizar, A., Militelli, M., Guerrero, R., 2008. Distribution of *Micopogonias Furnieri* at different maturity stages along an estuarine gradient and in relation to environmental factors. Journal of the Marine Biological Association of the United Kingdom 88 (1), 175–181.
Lasta, C., 1995. La Bahía Samborombón: zona de desove y cría de peces. Tesis Doctoral. Universidad Nacional de La Plata. 304 pp.
López Laborde, J., 1987. Distribución de sedimentos superficiales de fondo del Río de la Plata Exterior y Plataforma adyacente. Investigaciones Oceanológicas 1 (1), 19–30.
López Laborde, J., 1997. Marco geomorfológico y geológico del Río de la Plata, en The Río de la Plata: an Environmental Review, Wells, Daborn (Eds.), An ECOPLATA project Background Report, Dalhousie University, 248 p.
López Laborde, J., Nagy, G.J., 1999. Hydrography and sediment transport characteristics of the Río de la Plata: a review. In: Perillo, G.M.E., Piccolo, M.C., Pino, M. (Eds.), Estuaries of South America: Their geomorphology and dynamics. Springer, pp. 133–160.
Macchi, G.J., Acha, E.M., Lasta, C.A., 1996. Desove y fecundidad de la corvina rubia (Micropogonias furnieri Desmarest, 1823) del estuario del Rio de la Plata, Argentina. Boletín del Instituto Español de Oceanografía 12 (2). (99.113).
Meccia, V.L., Simionato, C.G., Fiore, M.M.E., D'Onofrio, E., Dragani, W.C., 2009. Sea surface height variability in the Río de la Plata estuary from synoptic to interannual scales: results of numerical simulations. Estuarine, Coastal and Shelf Science 85 (2), 327–343.
Meccia, V.L., Simionato, C.G., Guerrero, R., 2013. The Río de la Plata estuary response to wind variability in synoptic time scale: salinity fields and breakdown and reconstruction of the salt wedge structure. Journal of Coastal Research 29 (1), 61–77, http://dx.doi.org/10.2112/JCOASTRES-D-11-00063.1.
Miller, R.L., McKee, B.A., 2004. Using MODIS Terra 250 m imagery to map concentration of total suspended matter in coastal waters. Remote Sensing of Environment 93, 259–266.
Minetti, J.L., Vargas, W.M., 1990. Comportamiento del borde anticiclónico subtropical en Sudamérica II Parte. Revista de Geofisica 33, 177–190.
Morala, L., Serrano, A., García, J.A., 2003. Detecting quasi-oscillations in the monthly precipitation regimes of the Iberian Peninsula. Annales Geophysicae 21, 819–832.
Nagy, J.G., Martinez, C.M., Caffera, R.M., Pedralozza, G., Forbes, E.A., Perdomo, A.C., Laborde, J.L., 1997. The hydrological and climatic setting of the Río de la Plata. In " The Río de la Plata, an Environmental Review", An Eco-Plata Project Background Report, Dalhousie University, Halifax, Nova Scotia, pp. 17–68.
Nechad, B., Ruddick, K.G., Park, Y., 2010. Calibration and validation of a generic multisensor algorithm for mapping of total suspended matter in turbid waters. Remote Sensing in Environment 114 (4), 854–866.
O'Connor, W.P., 1991. A numerical model of tides and storm surges in the Río de la Plata estuary. Continental Shelf Research 11, 1491–1508.
Ottman, F., Urien, C.M., 1965. La melange des eaux douces et marines dans le Río de la Plata. Cahiers Oceanographiques 17, 213–234.
Ottman, F., Urien, C.M., 1966. Sur quelques problemes sedimentologiques dans le Río de la Plata. Revue de Géographie Physique et Géologie Dynamique 8, 209–224.
Parker, G., Cavalloto, J.L., Marcolini, S., Violante, R., 1986a. Los registros acústicos en la diferenciación de sedimentos subácueos actuales (Río de la Plata). 1er Reunión de Sedimentología Argentina, 32–44.
Parker, G., Cavalloto, J.L., Marcolini, S., Violante, R., 1986b. Transporte y dispersión de los sedimentos actuales del Río de la Plata (análisis de texturas). 1er Reunión de Sedimentología Argentina, 38–41.
Parker, G., Marcolini, J., Cavalloto, J., Violante, R., 1987. Modelo esquemático de dispersión de sedimentos en el Río de la Plata. Ciencia y Tecnología del Agua 1 (4), 68–80.
Parker, G., López Laborde, J., 1988. Morfología y variaciones morfológicas del lecho del Río de la Plata. En: SHIN – SOHMA. (Divs. Geología Marina). In: Proceedings of the "Estudio para la Evaluación de la Contaminación en el Río de la Plata", Inf. Téc. No. 4, Tarea 2.1.3.
Parker, G., López Laborde, J., 1989. Aspectos geológicos. En: CARP-SHIN-SOHMA (Ed.) "Estudio para la Evaluación de la Contaminación en el Río de la Plata", Informe de Avance a la Comisión Administradora del Río de La Plata, pp. 1–72.
Petus, C., Chust, G., Gohin, F., Doxaran, D., Froidefond, J.M., Sagarminaga, Y., 2010. Estimating turbidity and total suspended matter in the Adour River plume (South Bay of Biscay) using MODIS 250-m imagery. Continental Shelf Research 30, 379–392.
Robertson, A.W., Mechoso, C.R., 1998. Interannual and decadal cycles in river flows of southeastern South America. Journal of Climate 11, 2570–2581.
Rodrigues, K.A., 2005. Biología reproductiva de la saraquita, Ramnogaster arcuata del estuario del Río de la Plata. MS Thesis, University of Mar del Plata, Argentina, 40 pp.
Simionato, C.G., Nuñez, M.N., Engel, M., 2001. The salinity front of the Río de la Plata - a numerical case study for winter and summer conditions. Geophysical Research Letters 28 (13), 2641–2644.

Simionato, C.G., Dragani, W.C., Nuñez, M.N., Engel, M., 2004a. A set of 3-D nested models for tidal propagation from the Argentinean Continental Shelf to the Río de la Plata estuary: Part I, M_2. Journal of Coastal Research 20 (3), 893–912.

Simionato, C.G., Dragani, W.C., Meccia, V.L., Nuñez, M.N., 2004b. A numerical study of the barotropic circularion of the Río de la Plata Estuary: sensitivity to bathymetry, Earth rotation and low frequency wind variability. Estuarine, Coastal and Shelf Science 61, 261–273.

Simionato, C.G., Vera, C.S., Siegismund, F., 2005a. Surface wind variability on seasonal and interannual scales over Río de la Plata area. Journal of Coastal Research 21, 770–783.

Simionato, C.G., Meccia, V.L., Dragani, W.C., Nuñez, M.N., 2005b. Barotropic tide and baroclinic waves observations in the Río de la Plata Estuary. Journal of Geophysical Research 110, C06008, http://dx.doi.org/10.1029/2004JC002842.

Simionato, C.G., Meccia, V.L., Dragani, W.C., Guerrero, R., Nuñez, M.N., 2006. The Río de la Plata Estuary response to wind variability in synoptic to intra-seasonal scales: barotrópica response. Journal of Geophysical Research 111, C09031, http://dx.doi.org/10.1029/2005JC003297.

Simionato, C.G., Meccia, V.L., Guerrero, R.A., Dragani, W.C., Nuñez, M.N., 2007. The Río de la Plata estuary response to wind variability in synoptic to intra-seasonal scales: 2. Currents' vertical structure and its implications for the salt wedge structure. Journal of Geophysical Research 112, C07005, http://dx.doi.org/10.1029/2006JC003815.

Simionato, C.G., Berasategui, A., Meccia, V.L., Acha, M., Mianzán, 2008. Short time-scale wind forced variability in the Río de la Plata estuary and its role on ichthyoplankton retention. Estuarine, Coastal and Shelf Science 76 (2), 211–226, http://dx.doi.org/10.1016/j.ecss.2007.07.031.

Simionato, C.G., Meccia, V.L., Dragani, W.C., 2009. On the path of plumes of the Río de la Plata estuary main tributaries and their mixing time scales. Geoacta 34, 87–116.

Simionato, C.G., Luz Clara Tejedor, M., Campetella, C., Guerrero, R., Moreira, D., 2010. Patterns of sea surface temperature variability on seasonal to sub-annual scales at and off shore the Río de la Plata estuary. Continental Shelf Research , http://dx.doi.org/10.1016/j.csr.2010.09.012.

Simionato, C.G., Moreira, D., Piedra Cueva, I., Fossati, M., Guerrero, R., de los Campos, T., Balestrini, C., Cayocca, F., Gohin, F., Repecaud, M., 2011a. Proyecto FREPLATA – FFEM Modelado Numérico y Mediciones *in-situ* y Remotas de las Transferencias de Sedimentos Finos a través del Río de la Plata. Parte A: Adquisición de Datos. Frente Marítimo1015-323322, 109–136.

Simionato, C.G., Moreira, D., Re, M. and Fossati, M., 2011b. Estudio de la dinámica hidro-sedimentológica del Río de la Plata: observación y modelación numérica de los sedimentos finos. 109 pp., Published by Proyecto FREPLATA, CTMFM-CARP, ISBN 978-92-990052-9-3.

Snedden, G.A., Cable, J.E., Swarzenski, C., Swenson, E., 2007. Sediment discharge into a subsiding Louisiana deltaic estuary through a Mississippi River diversion. Estuarine, Coastal and Shelf Science0272-771471, 181–193, http://dx.doi.org/10.1016/j.ecss.2006.06.035.

Sykes, P.A., Barciela, R.M., 2012. Assessment and development of a sediment model within an operational system. Journal of Geophysical Research 117, C04036, http://dx.doi.org/10.1029/2011JC007420.

Urien, C.M., 1966. Distribución de los sedimentos en el Río de la Plata Superior. Boletín Servicio de Hidrografía Naval 3, 197–203.

Urien, C.M., 1967. Los sedimentos modernos del Río de la Plata Exterior. Servicio de Hidrografía Naval, Argentina, Público H-106, 4, 113–213.

Urien, C.M., 1972. Río de la Plata Estuary environments. Geological Society of America Memoirs 133, 213–234.

Vera, C.S., Vigliarolo, P.K., Berbery, E.H., 2002. Cold season synoptic scale waves over subtropical South America. Monthly Weather Review 130, 684–699.